UCRL 2208 REV.

UNIVERSITY OF CALIFORNIA

Radiation Laboratory

TIME QUANTIZATION IN A FEEDBACK SYSTEM

TWO-WEEK LOAN COPY

This is a Library Circulating Copy which may be borrowed for two weeks. For a personal retention copy, call Tech. Info. Division, Ext. 5545

This report was prepared as an account of Government sponsored work. Neither the United States, nor the Commission, nor any person acting on behalf of the Commission:

A. Makes any warranty or representation, express or implied, with respect to the accuracy, completeness, or usefulness of the information contained in this report, or that the use of any information, apparatus, method, or process disclosed in this report may not infringe privately owned rights; or

B. Assumes any liabilities with respect to the use of, or for damages resulting from the use of any information, apparatus, method, or process disclosed in this report.

As used in the above, "person acting on behalf of the Commission" includes any employee or contractor of the Commission to the extent that such employee or contractor prepares, handles or distributes, or provides access to, any information pursuant to his employment or contract with the Commission.

DISCLAIMER

This document was prepared as an account of work sponsored by the United States Government. While this document is believed to contain correct information, neither the United States Government nor any agency thereof, nor the Regents of the University of California, nor any of their employees, makes any warranty, express or implied, or assumes any legal responsibility for the accuracy, completeness, or usefulness of any information, apparatus, product, or process disclosed, or represents that its use would not infringe privately owned rights. Reference herein to any specific commercial product, process, or service by its trade name, trademark, manufacturer, or otherwise, does not necessarily constitute or imply its endorsement, recommendation, or favoring by the United States Government or any agency thereof, or the Regents of the University of California. The views and opinions of authors expressed herein do not necessarily state or reflect those of the United States Government or any agency thereof or the Regents of the University of California.

UCRL-2208 (Rev.)
Physics and Mathematics

UNIVERSITY OF CALIFORNIA

Radiation Laboratory
Berkeley, California

Contract No. W-7405-eng-48

TIME QUANTIZATION IN A FEEDBACK SYSTEM

John F. Waddell and Harold D. Morris

July 1957

Printed for the U.S. Atomic Energy Commission

TABLE OF CONTENTS

Abstract 5

1. Introduction 6

1.1 Summary of the pertinent literature to date 7
1.2 Statement of purpose 9

2. Mechanism of the sampling process 10

2.1 A physical description 10
2.2 Transfer properties 16
2.3 The output spectrum 18
2.4 The transfer function. 27

2.4.1 Behavior near odd multiples of half the sampling frequency 28
2.4.2 Behavior at multiples of sampling frequency . . . 31
2.4.3 Particularization to the clamped sampler. 32
2.4.4 Particularization to the impulse case 33

2.5 Sampler output corresponding to an arbitrary periodic input of period near $2/\nu_o$ 36

3. The problem of stability in a feedback loop 42

3.1 Conditions for the occurrence of oscillations having a period of $2/\nu_o$ 43
3.2 Application to the clamped, and impulse cases 51
3.3 General case of feedback oscillations 51

4. Experimental verification of the theory 55

4.1 Apparatus and methodology 55
4.2 Measurement of the transfer function 56
4.3 Spectral analysis experiment 59
4.4 The closed-loop stability experiment 63
4.4.1 Description of the experiment 63
4.4.2 Data reductions 65
4.4.3 Critical gain prediction by transient analysis . . . 69
4.4.4 Application of the stability criterion 72
4.4.5 Tabulation and comparison of results 73

5. Conclusions 78

6. Achnowledgment 79

Appendix I. Waveform factor of a capacitively clamped sampler ('Droop'). 80

LIST OF FIGURES

1.1 A typical time-quantized feedback system 7

2.1 Illustrating clamped sampling for an input signal of arbitrary waveform . 10

2.2 Clamped sampler input and output for input frequency of 7/8 sampling frequency 12

2.3 Clamped sampler output for input signals of 1/8 and 7/8 sampling frequency, and spectrum of output in region below sampling frequency 13

2.4 Clamped sampler output for input frequency of 1/8 or 7/8 sampling frequency 14

2.5 Illustration of the effect of sampling phase upon clamped sampler output when input frequency is half the sampling frequency 16

2.6 Input and output of a sampler having some (arbitrary) pulse shape g(t) 21

2.7 Pulse train of Fig. 2.6a, and magnitude of the spectral density of a single pulse 23

2.8 Structure of sampler output spectrum 24

2.9 Result of an experimental attempt to detect cross-modulation 26

2.10 Partial transfer function of a perfect amplitude sampler of the clamped type 29

2.11 Complete transfer function for the clamped sampler in the first four orders, with interference structure occurring at $n\nu_o/2$ shown 33

2.12 Region below the first zero of the sampler transfer function of Fig. 2.11, showing mechanism of interference between spectral components of sampler output at half-sampling frequency 34

3.1 Feedback loop containing a sampler and elements whose transfer properties can be described by the function $KG(\omega)$. 44

3.2 Geometrical interpretation of the stability criterion of Eq. (3.20) for a hypothetical feedback loop, having a frequency characteristic $G(\omega)\ W(\omega)$ 50

4.1 The essential features of an amplitude sampler of the clamped type, using a capacitive clamp 55

4.2 Circuit diagram of model sampler used in experiments described in text 57

4.3 Magnitude of transfer function of clamped sampler, with experimental points measured from model sampler 58

4.4 Spectrum analysis experiment: deviation plots, nondiagonal terms . . 61

4.5 Behavior of the diagonal term of the deviation matrix shown as a function of the spectrum line measured 62

4.6 Sampler-RC feedback experiment: schematic wiring diagram 64

4.7 Sample-RC feedback experiment: closed-loop simplified schematic wiring diagram 66

4.8 Sampler-RC feedback experiment: open-loop simplified schematic wiring diagram 66

4.9 RC delay network with output shunting resistance R' 67

4.10 Oscillations at half the sampling frequency in a feedback loop whose frequency properties are determined by a simple RC low-pass filter section 71

4.11 Transfer function of RC phase-lag network, showing the three cases for which critical closed-loop gain measurements were made at half-sampling frequency 74

4.12 Transfer function of feedback loop, Case 1 showing partial sums to order 5/2, and limits 77

I-1 Sampling process, showing the origin of 'droop', or waveform factor 83

I-2 Sampling process for $v/v_o = 1/2$ 83

I-3 Sampling process for $v/v_o = 1/4$, with heavy line showing the equilibrium output 85

I-4 Resolution of waveform of Fig. I-3 into component similar waveforms 85

I-5 Waveform factor of a clamped sampler having a sampling 'efficiency' of 0.958 ('droop' of 4.2%) 87

TIME QUANTIZATION IN A FEEDBACK SYSTEM

John F. Waddell* and Harold D. Morris**

University of California Radiation Laboratory
Department of Physics, Berkeley, California

July 1957

ABSTRACT

This report discusses effects observed in a feedback system, otherwise linear, in which time is quantized (these systems are often termed "sampled-data" systems). The time-quantizer ("sampler"), the most important element in the system, is treated in detail as applying to any sort of sampling that can be approximated by a purely amplitude-sampling process.

Following a general physical description of amplitude-sampling, the output spectrum of an amplitude-sampler of arbitrary pulse shape is derived and discussed. On the basis of the spectral analysis, a linear transfer function is developed which is applicable, with certain important limitations, to signals of all frequencies. The behavior of this transfer function is discussed, and several cases are distinguished.

The problem of stability in a feedback loop is treated, with particular attention to the important type of oscillations that are here dubbed "sampling oscillations". A general criterion for stability is developed, which includes all possible oscillations. Mathematical and physical interpretation of the stability criterion is provided, and a procedure is devised for the solution of practical problems.

Experimental evidence is offered in support of the theoretical results, with good agreement. The theory is also checked by calculation of the behavior of a special case whose sampling oscillations are amenable to transient analysis; complete agreement between these calculations and the prediction of the theory is found to exist.

---

*Now at the University of California Radiation Laboratory, Department of Physics, Livermore, California.

**Now at Donner Scientific Company, Concord, California.

TIME QUANTIZATION IN A FEEDBACK SYSTEM

John F. Waddell and Harold D. Morris

University of California Radiation Laboratory
Department of Physics, Berkeley, California

July 1957

1. INTRODUCTION

This work treats some physical concepts useful in dealing with feedback systems having a quantized time-base. Such a situation arises when in an otherwise continuous-control feedback loop, some nonlinear element is inserted which imposes upon the system a quantization of time, or as it is usually called for convenience, a 'sampling' process. Whatever the means by which the time-quantizing element, or 'sampler' operates, the result is the same: time is divided into equal intervals, at the beginning of each of which the loop is closed, being opened once again before more than a small fraction of a time quantum has passed. The output of the sampler is a train of pulses, one for each quantum of time, which carry the information derived from the momentary loop closure. In the usual form of sampler, the envelope of the output pulse-train approximates the input signal. The analytical methods and concepts used here apply to any pulse shape, and with adaptation, to any type of sampling.

An example of a time-quantized feedback system is given in Fig. 1.1; in this scheme it is the error signal which is sampled. There is a number of possible variations of such a system which merely represent different arrangements of elements in the feedback loop. To these apply the same concepts and methods, even as to systems containing only passive elements.

There are a number of possible ways in which the sampling process may take place. One example is the small-signal behavior of an ignitron rectifier in which output voltage control is achieved by controlling the phase at which the individual tubes begin to conduct.

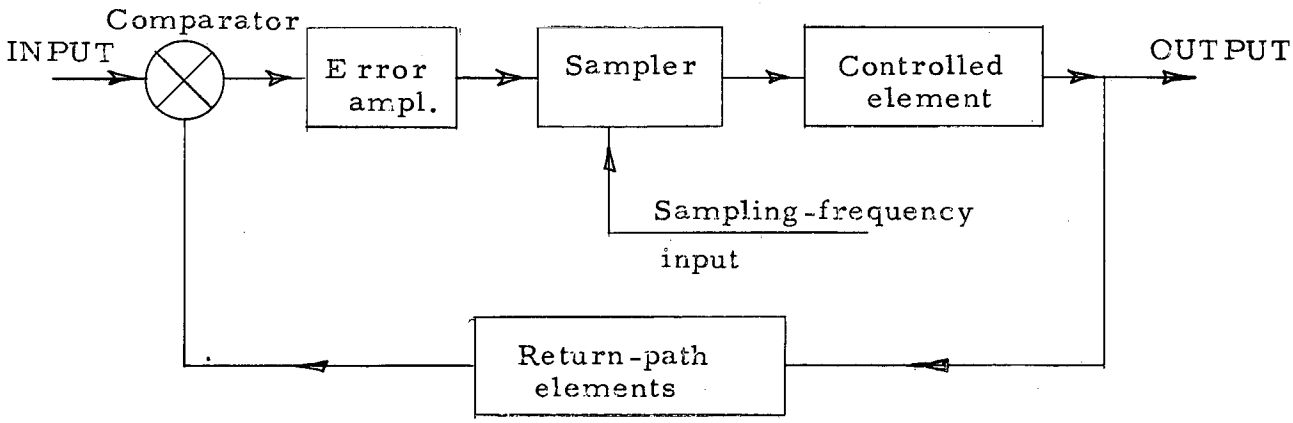

Fig. 1.1. A typical time-quantized feedback system.

1.1 Summary of the perinent literature to date. The earliest references in the field are those of MacColl,[1] and Hurewicz.[2] Each of these authors uses an approach based upon the 'Z-transformation' method, which has enjoyed almost universal popularity among writers in this field. The Z-transformation is a disguised Laplace transformation; the basis of the method is the use of sequences representing the values of input, output, and signals at other points in the feedback loop, at each instant of sampling.

The Z-transformation method thus involves calculation with knowledge of the pertinent signals only at the sampling instants, and with no knowledge of these signals between sampling instants; the method involves much in the way of mathematical abstraction, with an accompanying loss of a sense of physical reality, making physical interpretation of the theory a difficult business indeed. Its rewards are considerable notational simplification in an intrinsically 'messy' subject.

[1] MacColl, Fundamental Theory of Servomechanisms, Van Nostrand, 1954, (Ch. 10).

[2] Hurewicz, in James, Nichols, and Phillips (editors), Theory of Servomechanisms, M.I.T. Radiation Laboratory Series, Vol.25, McGraw, 1947.

Another point of view is that of Linvill, who takes a physical view of the problem in a very clear paper,[3] which treats the particular case of 'impulse'-sampling in detail. Linvill regards the use of any sampling pulse shape other than the impulse, or delta-function as being amenable to treatment as impulse-sampling plus linear filtering. This is approximately true in most common cases, but is not an applicable point of view when the sampler pulse is shaped by nonlinear or by active networks, or when the sampling is done by means other than purely amplitude-sampling. The ignitron rectifier case cited above provides an example. Linvill develops expressions for the sampler input and output spectra and time-functions, and uses these, and the fact that the spectrum of the impulse-sampler output is periodic in the sampling frequency to derive an expression for the output time-function of a feedback loop containing a sampler. An extension of Nyquist's stability criterion is implicit in his output equations, and he treats its application in the remainder of the paper.

The spectral (Laplace Transform) point of view was applied to feedback systems containing a digital computer by Salzer,[4] a student of Linvill.

A very clear review of the field as of 1951 was contributed by Ragazzini and Zadeh[5] who are exponents of the Z-transform method, and who undertake most successfully the task of relating the Z-transform method to the Laplace transform approach of Linvill. Their work is expository in nature, and is probably the most significant single contribution to date.

A paper by Lago and Truxal[6] concerns itself with the design of sampling systems, using the Z-transform method to treat the stability problem, and using open-loop impulse-response calculations to derive the response between sampling instants. This approach only applies, however, to impulse-sampling.

---

[3] Linvill, W.K., "Sampled-data Control Systems Studies through Comparison of Sampling with Amplitude Modulation", Trans. A.I.E.E. 70, 1779 (1951).

[4] Salzer, J.M., PhD. Thesis, M.I.T. (1951).

[5] Ragazzini, J.R., and Zadeh, L.A., "The analysis of Sampled-data Systems", Trans. A.I.E.E. 71, 225 (1952).

[6] Lago, G.V., and Truxal, J.G., "The Design of Sampled-data Feedback Systems", Trans. A.I.E.E. 73, 247 (1954).

In a paper based upon his Ph.D. thesis, Lago[7] reveals a discrepancy between the results of the Laplace and Z-transform methods and proceeds to resolve the question. In another contribution, Lago[8] outlines a method by which sampled-data systems can be synthesized, using the Z-transform method.

1.2 Statement of purpose. This work was undertaken to develop a theory of stability based upon the spectral approach, and to provide physical interpretation of the phenomena involved. In general we share the opinion of Linvill that the viewpoint which stresses frequency analysis lends itself most readily to physical interpretation. This work is intended to be of expository nature, to shed as much light as possible upon an intrinsically difficult subject, and to treat it in such a way as to expose the physical relationships which are hidden by the mathematical abstractions which characterize the other methods.

Along with the spectral point of view, we also carry out the analysis in terms of an arbitrary or generalized pulse shape, subject only to the requirement that its Fourier integral converge. Thus considerable generality is gained, in that applicability of the theory herein developed is not limited to cases where pulse shaping is performed by linear networks. The sampling process need not be a pure amplitude sampling process at all, but may be accomplished by any means which yields a sampled output proportional to the amplitude of the input signal at the sampling instants. The sampling method may be so complicated as to defy any reasonable analytical explanation; nonetheless, the theory developed here may be applied as long as the networks containing the sampling process are susceptible to transfer-function measurement and to determination of output spectrum.

---

[7] Lago, G.V., "Additions to Sampled-data Theory", Proc. National Electronics Conference 10, 758 (1954).

[8] Lago, G.V. "A Synthesis Procedure for Sampled-data Systems", Proc. National Electronics Conference 11, 351 (1955).

2. MECHANISM OF THE SAMPLING PROCESS

The sampling process consists in the generation of a train of pulses which represents the amplitude of the input signal at the beginning of each quantum of time. The "clamped" sampling process (square-pulse sampling) is described pictorially in Fig. 2.1.

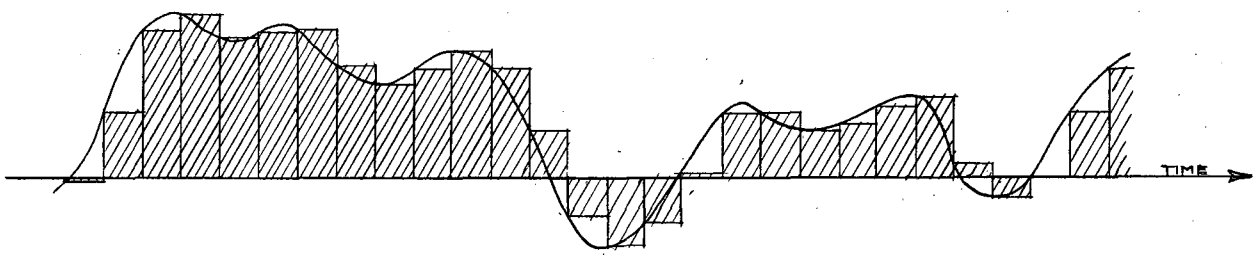

Fig. 2.1. Illustrating clamped sampling for an input signal of arbitrary waveform.

The discussion to follow will concern itself principally with the transmission of a sinusoidal input signal of arbitrary frequency having unit amplitude, as is usual in discussions of linear processes. The most that can be said of the sampling process is that it is a 'linear' modulation process, i.e., the process is one of modulation in which the nonlinearity exists between the sampling frequency signal and the input signal components, but not between the input components themselves. Thus to an input signal component having some frequency ν there corresponds an output component of the same frequency whose amplitude is proportional to that of the corresponding input component.

2.1 A physical description. For an input signal whose frequency is very small compared with the sampling frequency, time quantization has negligible effect, and the ordinary linear analysis is reasonably satisfactory. As the frequency of the input signal increases, so as to no longer be much smaller than the sampling frequency, the effects of sampling become noticeable, and the degree of approximation to which the linear analysis applies becomes less.

As the input frequency approaches the sampling frequency, sampling effects become predominant, and the ordinary feedback theory fails in several important respects. How this comes about is perhaps best explained from a purely physical point of view. For convenience, the discussion of this section will be particularized to the case of "clamped" sampling.

To being with, let us consider the case of an input signal whose frequency is exactly the sampling frequency, i.e., let the input signal be sampled at its own frequency; then the output can contain only a constant amplitude (zero frequency) term. The amplitude of the output then depends only upon the phase at which sampling occurs, and accordingly can take on any value of amplitude which might be instantaneously assumed by the input signal during a period. Now suppose that the input signal frequency is somewhat below sampling frequency (which we will call ν_o). Sampling will take place at intervals of somewhat less than a period of the input signal. The output will accordingly be a train of square pulses of length nearly equal to a period. This situation is shown in Fig. 2.2. The reader should take particular note of the fact that by far the largest spectral component of the output has a frequency much lower than that of the input. Actually, as will be shown later, the low frequency is the difference between input and sampling frequencies. There will also be a small component of frequency equal to that of the input signal, and smaller components whose frequencies are greater than the sampling frequency.

One might now ask what the situation would be were the frequency of the input signal to have the lower value (i.e., lie close to zero). Figure 2.3 shows the outputs due to input signals of unit amplitude and frequencies of $\nu_o/8$ and $7\nu_o/8$ to be identical (at least insofar as the accuracy of geometrical construction permits such a conclusion). Also shown in Fig. 2.3 are the output spectral components having these two frequencies, accurately plotted from results to be shown in subsequent paragraphs. These are the largest components, and their sum is plotted in Fig. 2.4 simply as a matter of interest.

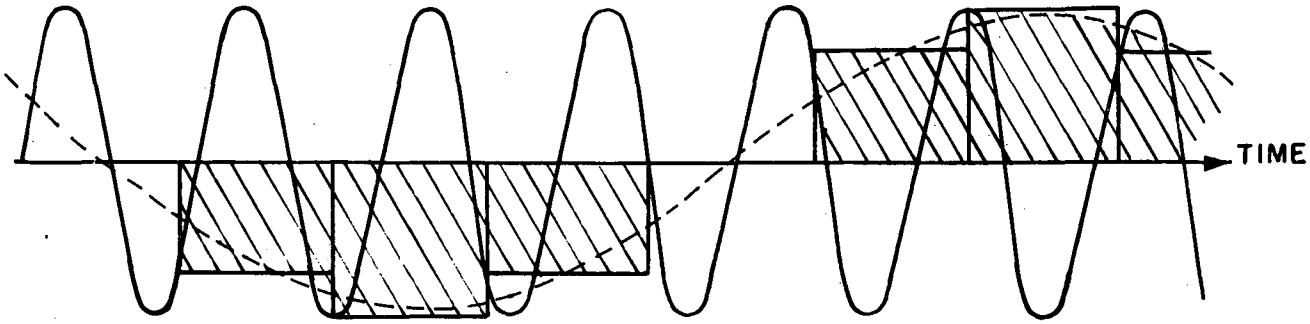

Fig. 2.2 Clamped sampler input and output for input frequency of 7/8 sampling frequency. Note the generation of a low frequency (difference frequency) component nearly as large in amplitude as the input signal itself.

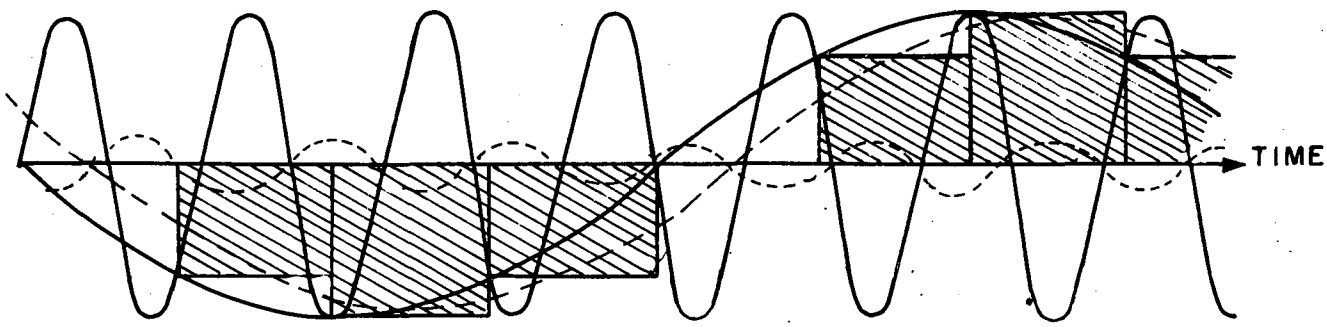

Fig. 2.3 Clamped sampler output for input signals (solid lines) of 1/8 and 7/8 sampling frequency, and spectrum of output (i.e., output components) in the region below sampling frequency.

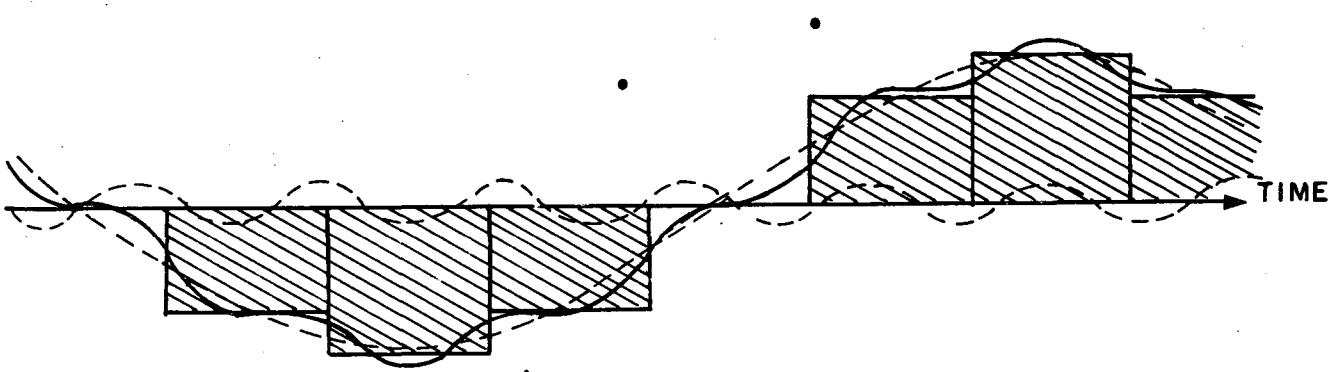

Fig. 2.4 Clamped sampler output for input frequency of 1/8 or 7/8 sampling frequency. Components of the output having those frequencies are shown, together with their sum.

It is possible now to form a picture of what the output spectrum looks like in the range of frequencies less than ν_o. Given an input signal of unit amplitude and variable frequency, for input frequency close to zero the output will contain a component of the same frequency whose amplitude will be close to unity. A difference frequency component will exist having an amplitude close to zero. As frequency of input (ν) approaches zero as a limit, output component amplitudes approach, as limits, unity for frequency ν, zero for frequency $\nu_o - \nu$. As ν increases, amplitude of the component of input frequency decreases, and amplitude of the difference frequency component increases.

At this point it is well to inquire into the happenings at half-sampling frequency, where the input and difference frequencies are equal. As for the case between input and sampling frequencies, magnitude of the output depends upon phase of the input signal at sampling instants, a situation illustrated graphically in Fig. 2.5. If the input frequency were slightly different from $\nu_o/2$, the square wave train would grow slowly to maximum value, then shrink to νero, then grow with opposite phase, pass maximum value, and shrink again, etc. This is suggestive of an interference phenomenon, a concept which will be touched upon at length in subsequent paragraphs. One may see the plausibility of the interference argument, when one considers that were the input and difference frequency components of equal magnitude at half-sampling frequency, interference between these (since the phase of each should depend upon sampling phase) could account for reinforcement or cancellation of the $\nu_o/2$ component of the output according to whether sampling phase was favorable or unfavorable. As will be seen subsequently, at $\nu_o/2$, the two components in question are indeed of equal magnitude, a fact which has important bearing upon the transfer properties of the sampling device.

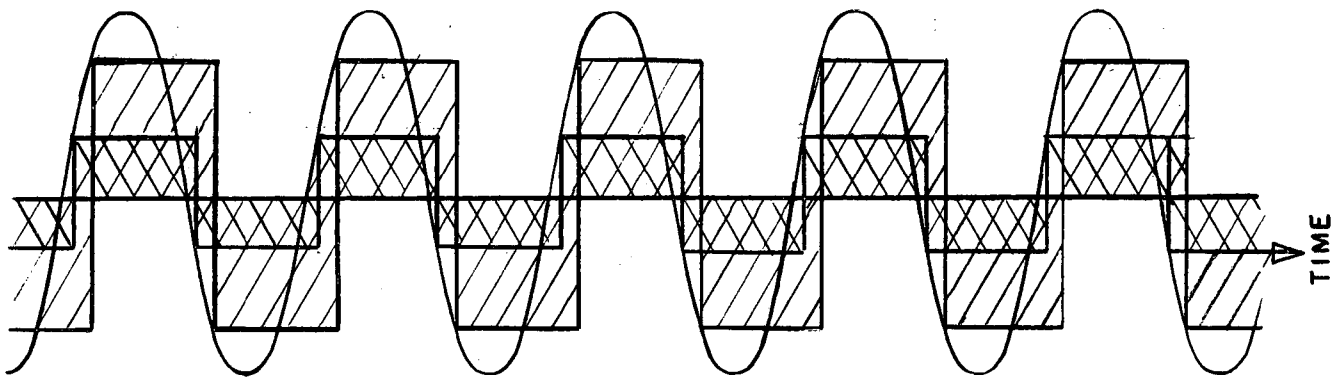

Fig. 2.5. Illustration of the effect of sampling phase upon clamped sampler output when input frequency is half the sampling frequency.

Next consider the cases in which $\nu = n\nu_o/2$ for $n > 2$. For the even case ($\nu = m\nu_o$) it is obvious that the result is identical with the case $m = 1$, where the output has zero frequency with amplitude dependent upon phase at which sampling occurs. The only difference now is that sampling occurs every m periods of the signal. A similar relation holds for the half-multiples, $\nu = (2m-1)\,\nu_o/2 = (m - 1/2)\,\nu_o$. Here a train of square waves occurs, period being $2/\nu_o$, sampling occuring every $(m - 1/2)$ periods of the signal. As will be brought out later in treatment, the sum-and-difference frequency pattern repeats in every band of width ν_o sec^{-1}; i.e., with every multiple of sampling frequency, including zero, there is associated a pair of spectrum lines of frequencies $m\nu_o + \nu$ and $(m + 1)\nu_o - \nu$. Physical behavior of the output is similar in the higher orders to that noted for the zeroth order, with the same interference behavior at $(m - 1/2)\nu_o$ and the zero-beat phenomena at $m\nu_o$. These effects have been observed experimentally on a physical sampler up to approximately the 50th order, at which time imperfections in the sampler caused difficulty in the observations.

2.2 Transfer properties. In discussing the transfer properties of a sampler, interest lies almost exclusively in the region between zero and sampling frequency. By the term 'transfer properties' we mean the relationships existing between the input signal (a sinusoid of frequency ν) and that component of the output spectrum having the same frequency ν.

This relationship may conveniently be expressed in terms of a 'transfer function' which is the complex ratio of output to input (considering only the output component having input frequency).

The term 'transfer function' is used by most writers in feedback theory to describe something quite different from what is dealt with here.[9] In ordinary feedback theory, the transfer function of a network is the ratio of the transform of the output time-function to that of the input for any arbitrary input function. The transform may be any operational transform: Laplace, Fourier, or Heaviside. For a linear passive network, the definition of 'transfer function' to be used in this work agrees with the customary definition with the Fourier Transform used. This function is called by some writers the 'frequency transfer function'. In this sense, the transfer function is a 'spectral modifying function' wherein the spectrum of the input is modified only by changes in amplitude and phase of the spectral components, these changes being a function of frequency of the component operated upon (thence the term 'operator' applied by some authors). Indeed, the above is an embodiment of the principle of superposition, in that the output spectrum contains no components having a frequency not present in the input.

In the time-quantized case, however, the principle of superposition holds in another sense, namely that the output spectrum due to an input spectrum made up of a series, or superposition of spectra, is the superposition of the output spectra due to each of the individual inputs. This will be demonstrated in a later section. The sampler is a device having two inputs and one output; nonlinearity occurs between the signals entering the two inputs. There is, however, no nonlinearity between two signals simultaneously applied to the 'signal input', or 'THE' input.

It is readily seen, therefore, that no unique transfer function exists in the transform sense. This is merely another way of stating that in general, the output waveform is different from the input waveform, and no function can be written down which expresses the ratio of the output spectrum to that of the input, excepting in a purely symbolic way.

---

[9] Cf. Greenwood, Holdam, and MacRae, "Electronic Instruments", M.I.T. Rad. Lab. Series, Vol. 21, p. 230 et. seq; or James, Nichols, and Phillips, reference 2, p. 58 et. seq.

The transfer function one thus obtains is dependent upon the input waveform, hence is not unique to the sampler alone.

In preceding paragraphs the general nature of the amplitude of the transfer function has been established as a monotone decreasing function having unit amplitude at zero frequency and zero amplitude at ν_o. A clue to the nature of the phase function may be found in Fig. 2.1. Disregarding the distortion introduced in the rapidly changing parts of the signal waveform by sampling at insufficiently large frequency, it seems reasonable to conclude that a constant delay of approximately half a sampling period occurs. Again, reference to Fig. 2.3 indicates the correctness of such a conclusion at the lower frequencies, although little can be said regarding frequencies in the region near ν_o. Thus in the lower range there is reason to conclude that the sampler is, or is nearly, a constant-delay (linear phase) device. Proof of this conclusion must depend upon mathematical analysis of the output spectrum, when it will appear that indeed the phase of any sampler is linear (in a 'sawtooth' fashion) for the entire frequency range, zero to infinity.

It is, of course, the transfer function of a sampler which is all-important in considering such a device as part of a feedback loop, hence this paper is devoted principally to a discussion of these transfer properties. Based upon physical reasoning a picture has been drawn of this function, on which only one blot appears, aside from waveform distortion, namely that at half-sampling frequency there is a discontinuity in behavior. This is of course due to the fact that $\nu_o/2$ is the only frequency for which $\nu_o - \nu = \nu$. Further discussion is best postponed until a quantitative account of the output spectrum and its salient features has been rendered, except to remark that at $\nu_o/2$ one might expect the sampler to be a poor risk in a feedback loop.

2.3 The output spectrum. In a discussion of the output spectrum resulting from a monochromatic input one tacitly implies belief in the applicability of the Principle of Superposition. To do this for a nonlinear device calls up a need for justification, which may be argued for on the basis of physical reasoning, and in support of which experimental evidence is offered. The sampler can be thought of as a 'linear modulator', i.e., a device in which one input (sampling frequency) is modulated by another input (which we term

'THE' input). The question is whether or not any cross-modulation effects may exist between spectral components of 'THE' input.

As an examination of the equations describing the output spectrum for a signal of generalized waveform will show, no cross-modulation is theoretically possible. This conclusion is borne out experimentally. Quantitative discussion will be presented later in this section (see Eq. 2.8 and Fig. 2.9, below).

As mentioned previously, the interest in this paper lies primarily with the sampler of 'clamped' type; however, in deriving expressions for the output spectrum there is only complication to be gained from restricting generality of the pulse shape. Accordingly, the more general case will be discussed.

An excellent discussion of the factors affecting spectral composition of the sampler output is given by Bennett,[10] who deals with the 'flat' spectrum resulting from 'instantaneous' sampling (sampling pulses are modulated delta-functions). For pulses of finite length the spectrum is modified by an 'aperture effect' which is a function of pulse shape and length. The treatment is very elegant, and lends itself well to discussion in verbal terms without loss of mathematical or physical essence. The most concise expression for the output spectrum is, however, the result of Kleene,[11] whose paper is a mathematical analysis yielding the output of a sampler having generalized pulse shape, assuming a generalized input waveform. Those results will be used, and enlarged upon, in this work.

Another method of deriving expressions for the output spectrum consists merely in assuming that the input signal is monochromatic, and that the ratio of signal frequency to sampling frequency is a rational number. Computable forms have been derived from which the transfer function was calculated on a discrete set. Justification for such a procedure stems from the density property of rational numbers, hence for the result not to represent the transfer function of the sampler for incommensurable frequencies would mean that the function was totally discontinuous. Needless to say, an assumption of pulse waveform is necessary, hence there is considerable lack of generality in this sort of analysis. Moreover although the form of the results lends itself to numerical calculation, it is not very revealing to inspection regarding functional form of the spectral distribution.

[10] Bennett, W. R., "Spectra of Quantized Signals", Bell System Technical Journal 27, 446 (1948).

[11] Kleene, S. C., "Analysis of Lengthening of Modulated Repetitive Pulses", Proc. IRE 35, 1049 (1947).

Let there be given, then, a sampler whose pulse shape g(t) is arbitrary, save that its Fourier integral converges. An example of such a waveform is provided in Fig. 2.6a, which depicts the unmodulated output of a sampler (output for no signal input) as a function of time, t. The sequence of instants marking the beginning of each sampling period we call $\{t_k\}$, i.e., $\{t_k\} = \{k/\nu_o\}$, the sequence of sampling instants.

Assume that the input signal f(t) possesses an enumerable set of spectrum lines, implying that the input can be expressed as the sum of a finite, or enumerably infinite, set of periodic functions. Thus, we can express f(t) as a sum of Fourier series,

$$f(t) = \sum_{s=1}^{\infty} \sum_{m=-\infty}^{\infty} c_{ms} e^{2\pi i m \nu_s t} \tag{2.1}$$

where $1/\nu_s$ is the period of the sth periodic component of f(t).

Now by definition of the sampling process, an example of which is provided in Fig. 2.6b, the output of the sampler is

$$F(t) = f(\{t_k\})\, g(t - \{t_k\}) \tag{2.2}$$

consisting of the pulse train $g(t - \{t_k\})$ modulated by the sequence of input values at the sampling instants, $f(\{t_k\})$.

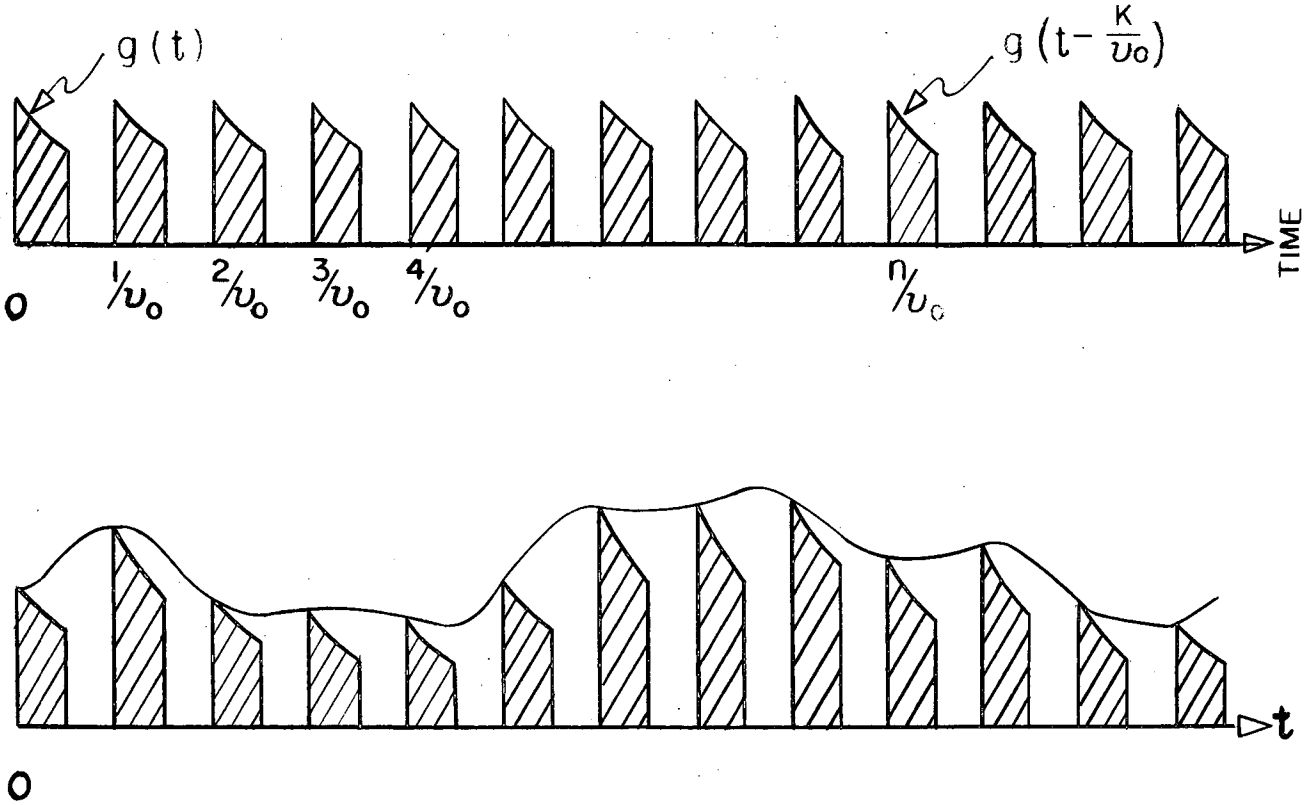

Fig. 2.6. Input and output of a sampler having some (arbitrary) pulse shape g(t)

(a) Unmodulated pulse train.

(b) Modulated pulse train F(t) (shown cross-hatched), with modulating input function f(t) (solid-line curve).

When (2.1) is written for the sequence $\{t_k\}$, and substituted into (2.2) with suitable transformations,[11] the result is

$$F(t) = \sum_{s=1}^{\infty} \sum_{m=-\infty}^{\infty} \sum_{m=-\infty}^{\infty} c_{ms} W(n\nu_o + m\nu_s) e^{2\pi i(n\nu_o + m\nu_s)t} \qquad (2.3)$$

[11] Kleene, op. cit.

where m and n are integers, and

$$W(\nu) = \nu_o \int_o^{1/\nu_o} g(t)\, e^{-2\pi i \nu t}\, dt \tag{2.4}$$

Here the nature of the output spectrum becomes apparent: that there are spectrum lines for all positive and negative (integral) values of m and n, at $n\nu_o + m\nu_s$. The complete spectrum of the input signal is transposed in frequency to cluster about each integral multiple ('harmonic') of the sampling frequency. The entire spectrum is modified by that of the single sampling pulse - i.e., each spectral component is modified by the Fourier transform of the sampling pulse, evaluated at the frequency of the line in question. Illustration of the above is given in Figs. 2.7 and 2.8.

In the case where the input has only one spectrum line in the positive frequency region (and one in the negative region) the relations take the form

$$f(t) = a \cos(2\pi\nu t) \tag{2.5}$$

or

$$f(t) = \frac{a}{2}\, e^{2\pi i \nu t} + \frac{a}{2}\, e^{-2\pi i \nu t} \tag{2.6}$$

Thus

$$F(t) = \sum_{n=-\infty}^{\infty} \frac{a}{2} \left[W(n\nu_o - \nu) e^{2\pi i (n\nu_o - \nu)t} + W(n\nu_o + \nu) e^{2\pi i (n\nu_o + \nu)t} \right] \tag{2.7}$$

One sees now that each integral multiple of ν_o has 'sidebands' differing from $n\nu_o$ by $\pm\,\nu$.

It is of interest to see what happens to the spectrum as input frequency is varied from zero upward to many times the sampling frequency. As the input frequency term ν starts from zero, the difference frequency term $\nu_o - \nu$ starts down from ν_o, and a set of sum-frequency terms $n\nu_o + \nu$ and of difference-frequency terms $(n+1)\nu_o - \nu$ approach each other in every interval of width ν_o. Each term is of course modified by $W(\nu)$.

As the input-frequency term comes to the value $\nu_o/2$, all of the sum and difference terms in each interval of width ν_o coalesce. When ν becomes larger than $\nu_o/2$, the spectrum lines change roles (as though they had 'passed' each other at the moment of coalescence), behavior of the

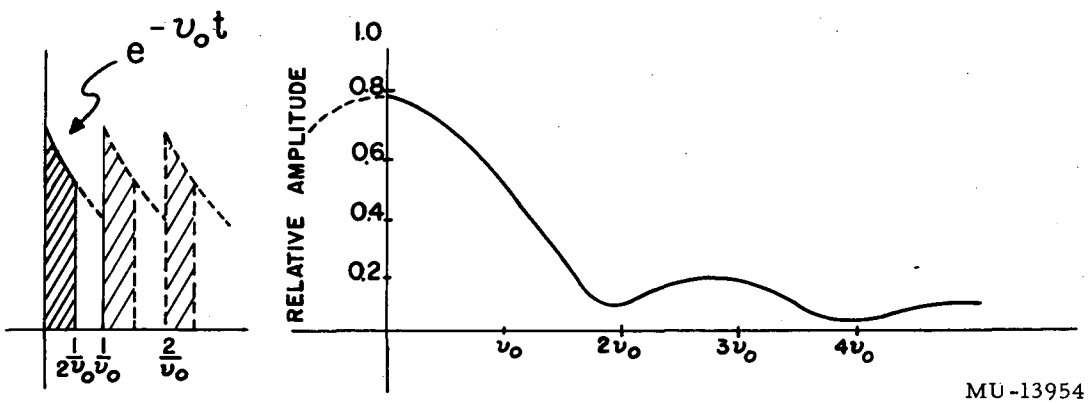

Fig. 2.7. Pulse train of Fig. 2.6a and magnitude of the spectral density (Fourier transform) of a single pulse (positive-frequency portion).

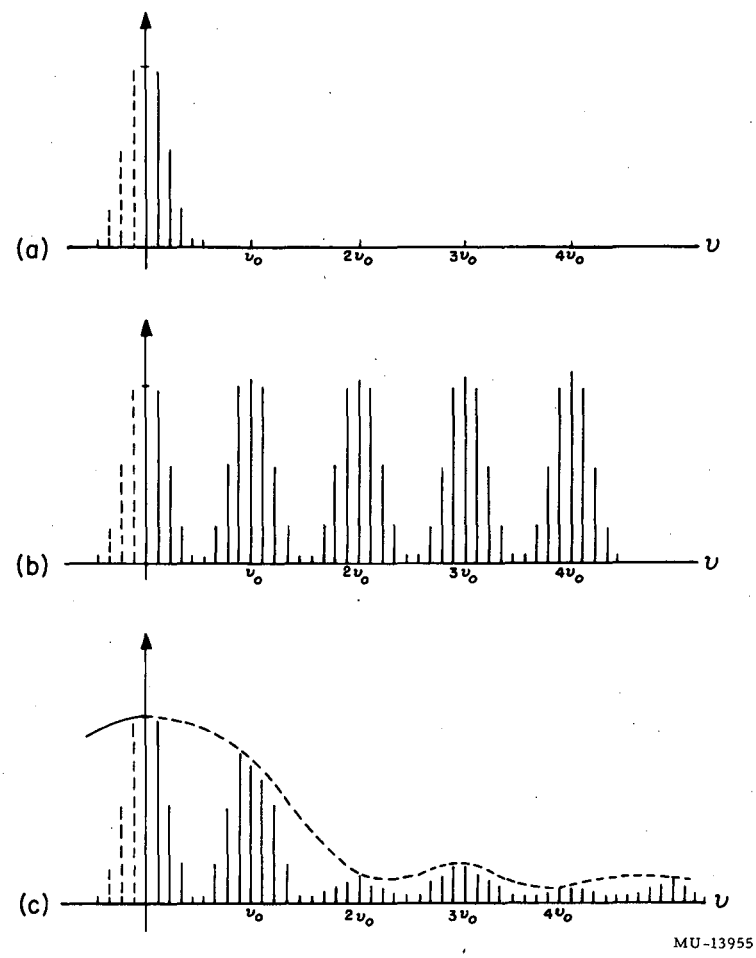

Fig. 2.8. Structure of sampler output spectrum.
(a) Amplitude spectrum of some arbitrary input signal.
(b) Input signal spectrum transposed to multiples of the sampling frequency. (This is not the output spectrum.)
(c) Input signal transposed and modified by spectrum of sampling pulse. Only amplitude is shown, of course. (This is the output spectrum).

spectrum being symmetrical about $\nu_o/2$. When ν is any integral multiple of ν_o the spectrum is identical to that for $\nu = 0$. Indeed, inspection of Eq. (2.7) shows that the same spectrum results for a unit amplitude input applied, having the frequency of any one of the spectrum lines. To illustrate the effects mentioned above, reference is made to Figs. 2.2 to 2.5.

One further effect is left to be explored, namely the possibility of cross-modulation. In equation (2.3) we let the index s take on the values 1, 2, and m the values ± 1 which correspond to an input signal consisting of two equal sinusoids of frequencies ν_1 and ν_2, thus:

$$F(t) = C \sum_{n=-\infty}^{\infty} \Big[W(n\nu_o - \nu_1) e^{2\pi i (n\nu_o - \nu_1)t} + W(n\nu_o + \nu_1) e^{2\pi i (n\nu_o + \nu_1)t} + W(n\nu_o - \nu_2) e^{2\pi i (n\nu_o - \nu_2)t} + W(n\nu_o + \nu_2) e^{2\pi i (n\nu_o + \nu_2)t} \Big], \tag{2.8}$$

since we have $C_{-1s} = C_{1s} = C_s = C_1 = C_2 = C$. The result being a linear combination of terms in each of the frequencies ν_1 and ν_2 separately, and having no terms of frequency $\nu_1 \pm \nu_2$ or of any other combination of ν_1 and ν_2, we are led to the obvious conclusion that cross-modulation does not occur. Hence the term 'linear modulation', used previously. It is thus seen that the principle of superposition has been correctly applied to the sampling process.

The experimental verification of the above result, mentioned previously in this section, is presented herewith. The laboratory model clamped sampler was used, this model being described in Section 4.1. An input signal whose amplitude was independent of frequency was used. The corresponding output signal was normalized at zero frequency.

In the experiment, the input was composed of two components, having a fixed difference in frequency. The input frequencies were ranged through several values between zero and ν_o, one case 'straddling' half-sampling frequency $(\nu_o/2)$. The difference frequency was chosen as $0.04\ \nu_o$, a feasible but small value well within the pass-band of the spectrum analyzer. Exploration was made of the region $0 < \nu < \nu_o$, which is equivalent to exploring the entire frequency axis, as pointed out in the discussion of the output spectrum. Results are shown in Fig. 2.9, it being noteworthy

that the magnitude of difference frequency component is never greater than 40 decibels below the input signal amplitude. Other components, i.e., the sum-frequency, and other linear combinations of ν_1 and ν_2, are smaller than the difference component. The presence of small cross-modulation products we therefore attribute to nonlinearity in the vacuum-tube networks associated with the model sampler.

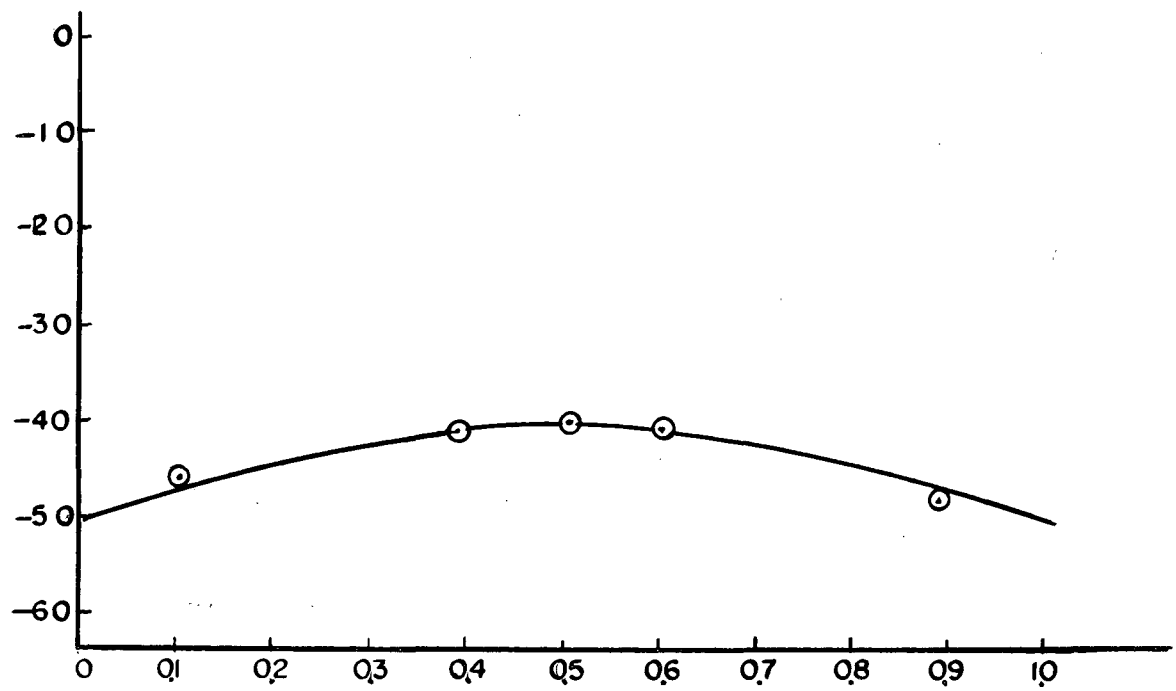

Fig. 2.9. Result of an attempt to detect cross-modulation. The quantity shown is the amplitude of the difference ("beat") frequency generated in the sampler and associated apparatus, resulting from an input signal consisting of two sinusoidal voltages each having unit amplitude, with frequency separation of $\nu_o/25$.

2.4. The transfer function. It is now that we turn to examine the behavior of a particular line of the output spectrum, that having the input frequency, as the input frequency is varied over the entire domain of real values. The input signal will be thought of as a real function with a positive real frequency, ν, expressible by Eq. (2.5). Since we are using complex Fourier series representation there are two spectrum lines, at $\pm\nu$ (i.e., $m = \pm 1$), as expressed in Eq. (2.6). The line having frequency ν is represented in Eq. (2.7) by the term in $+\nu$ for $n = 0$, namely $W(\nu)\exp(2\pi i\nu t)$. The coefficient of this term, $W(\nu)$, is the transfer function of the sampler everywhere except on the discrete set of frequencies $\nu = (2n - 1)\,\nu_o/2$, a case to be discussed in detail subsequently. $W(\nu)$ is defined by Eq. (2.4) which is assumed to be convergent, hence $W(\nu)$ is an analytic function of ν.

In the discussion to follow, it will be useful to have as an illustrative example a specific type of sampler. The clamped sampler provides, in the opinion of the authors, the most easily discussed form, both from a physical and mathematical standpoint. The discussion of the transfer function will, however, be kept in the most general possible terms, applicable to any pulse shape encountered in physical reality. Later in this section a further application of the principles will be made to the delta-function, or impulse-type sampler, which has some interesting properties.

In the case of the clamped sampler, the pulse is one of simple square shape, of duration equal to the repetition period. Thus, Eq. (2.4) integrates to

$$W(\nu) = e^{-i\pi\frac{\nu}{\nu_o}} \frac{\sin \pi\frac{\nu}{\nu_o}}{\pi\frac{\nu}{\nu_o}} \tag{2.9}$$

or,

$$\left|W(\nu)\right| = \left|\frac{\sin \pi\frac{\nu}{\nu_o}}{\pi\frac{\nu}{\nu_o}}\right| \tag{2.10}$$

$$\arg W(\nu) = -\pi\frac{\nu}{\nu_o} + \arg\left(\frac{\sin \pi\frac{\nu}{\nu_o}}{\pi\frac{\nu}{\nu_o}}\right) \tag{2.11}$$

Equation (2.11) embodies the linear phase property discussed previously; the function arg (sin u/u) being $-k\pi$, where k is the number of zeros of sin u/u which lie between 0 and u. The phase properties are an outgrowth of the pulse shape alone.

Figure 2.10 shows the locus of this transfer function in the complex plane for arg W $\leq$ 8π, i.e., for the first four orders of the spectrum.

The function $W(\nu)$ as described in equation (2.9) is everywhere single-valued and continuous in the domain of real frequencies. It has a zero at each point of the set $\nu = n\nu_o$ (n any integer > 0), implying that there is no output at sampling frequency or any integral multiple thereof greater than zero. Its curvature is continuous at the zeros as examination of (2.11) will show.

2.4.1. Behavior near odd multiples of half the sampling frequency. As has been previously mentioned, occurrence of the input frequency at any odd integral multiple of half-sampling frequency gives rise to discontinuous behavior of the transfer function. Physically, this result may be most easily ascribed to an interference between the sum and difference frequencies in each spectral order, since these lines coalesce in all orders when the input frequency becomes $(2n - 1)\ \nu_o/2$. That this interference actually occurs is shown in the analysis to follow.

The method is one of perturbation of the input frequency from any member of the set $(2n - 1)\ \nu_o/2$; recalling the property of the spectrum that identical spectra are obtained in response to unit inputs having the frequency of any line of the spectrum, we use the value $\nu_o/2$ for input frequency. Thus write Eq. (2.7), and change the index of summation from the multiple of sampling frequency to the spectral order, i.e., the kth interval lies between the $(k - 1)^{st}$ and the kth zeros. Then we have

$$F(t) = \sum_{k=-\infty}^{\infty} \frac{a}{2} \left\{ W\left[(k-1)\nu_o + \nu\right] e^{2\pi i\left[(k-1)\nu_o+\nu\right]t} + W\left[k\nu_o - \nu\right] e^{2\pi i\left[k\nu_o-\nu\right]t} \right\} \tag{2.12}$$

Let

$$\nu = \frac{\nu_o}{2} - \delta\nu \qquad \frac{\delta\nu}{\nu_o} <<< 1 \quad . \tag{2.13}$$

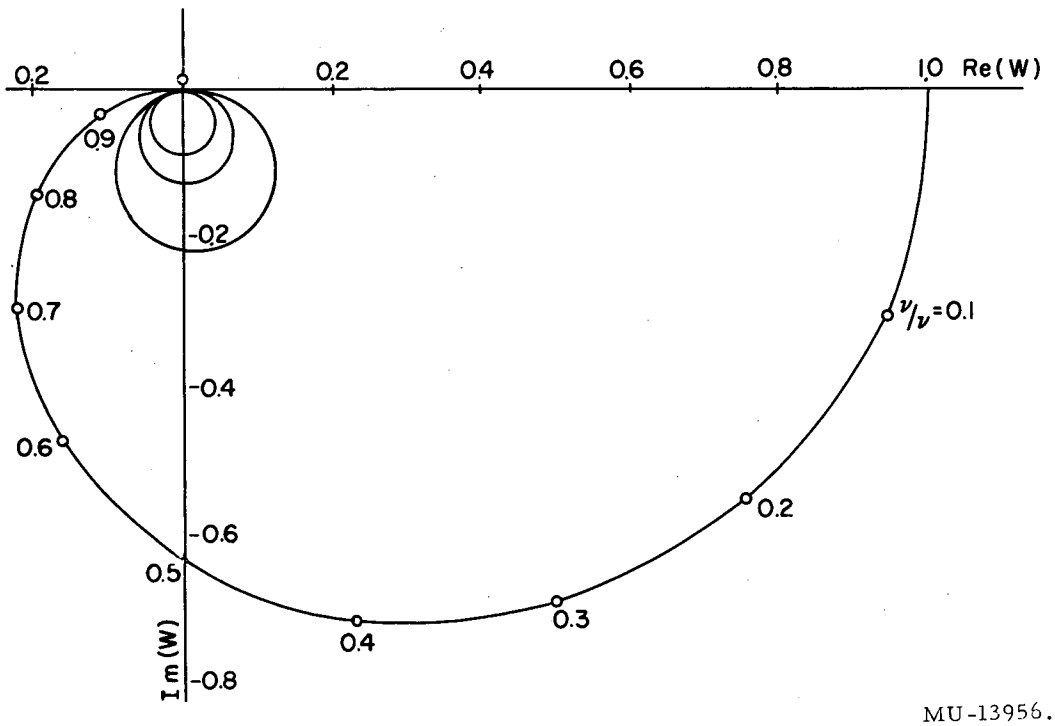

MU-13956.

Fig. 2.10. Partial transfer function of a perfect amplitude sampler of the clamped type. Numbers shown are the frequency normalized to sampling frequency. Only the first four orders of the function are shown.

Substituting (2.13) into (2.12), and simplifying the expressions for the frequencies, we have

$$F(t) = \sum_{k=-\infty}^{\infty} \frac{a}{2} \left\{ W\left[(k-1/2)\,\nu_o - \delta\nu\right] e^{2\pi i\left[(k-1/2)\nu_o - \delta\nu\right]t} + W\left[(k-1/2)\nu_o + \delta\nu\right] e^{2\pi i\left[(k-1/2)\nu_o + \delta\nu\right]t} \right\} \tag{2.14}$$

$W(\nu)$, being analytic, may be replaced by its Taylor expansion in the neighborhood of $(k-1/2)\nu_o$, k being any integer. In view of the restriction $\delta\nu/\nu << 1$, one may replace, in Eq. (2.14), $W\left[(k-1/2)\nu_o \mp \delta\nu\right]$ by the leading term $W\left[(k-1/2)\nu_o\right]$, and (2.14) becomes

$$F(t) = \sum_{k=-\infty}^{\infty} \frac{a}{2} W\left[(k-1/2)\nu_o\right] \left\{ e^{2\pi i\left[(k-1/2)\nu_o - \delta\nu\right]t} + e^{2\pi i\left[(k-1/2)\nu_o + \delta\nu\right]t} \right\} \tag{2.15}$$

Now we consider the behavior of each term separately--i.e., inquire into the goings and comings of each spectral order independently of the others. In so doing, phase is referred to the lower frequency line (that having the difference-frequency), with the result

$$F_k(t) \exp\left\{-2\pi i\left[(k-1/2)\nu_o - \delta\nu\right]t\right\} = \frac{a}{2} W\left[(k-1/2)\nu_o\right]\left[1 + e^{4\pi i\delta\nu t}\right] \tag{2.16}$$

In each order the output consists of the sum of two components which interfere, in the limit, when their frequencies are $k\,\nu_o/2$, to produce an output magnitude which is in accordance with the phase of sampling. If we allow the perturbation to remain, one sees the behavior very clearly. For <u>every order</u>, the rate of precession in phase of the upper component with respect to the lower has the same value, namely $2(2\pi\delta\nu)$. The time required for a precession through one period of the output is the same for all orders, irrespective of their frequency, noting that their frequencies are (perturbed) integral multiples of the signal frequency. Thus the output waveform grows from nothing to its maximum value, then shrinks again to nothing, the cycle

being repeated as long as the perturbation remains. Throughout all this process the waveform remains unchanged, since the interference is in each order of the same degree as in all the others, i.e., all the orders might be said to interfere in unison, or to the same degree, simultaneously. If at any time in the cycle here described the perturbation is removed, the output remains frozen at the condition then obtaining. Thus the exponent $2(2\pi\delta\nu t)$ is seen to be just twice the phase of sampling, the transfer function thus having period π with respect to the variable ϕ. Equation (2.16) may therefore be written, in the limit,

$$F_k(t)\exp\left[-2\pi i(k-1/2)\nu_o t\right] = \frac{a}{2}\, W\left[(k-1/2)\nu_o\right]\left[1+e^{2i\phi}\right] \tag{2.17}$$

where ϕ is the phase at which sampling occurs.

Equation (2.17) is the kth term of the series in Eq. (2.15) in the limit $\delta\nu = 0$; the output time-function is therefore

$$F(t) = \frac{a}{2}\,(1+e^{2i\phi})\sum_{k=-\infty}^{\infty} W\left[(k-1/2)\nu_o\right] e^{2\pi i\,(k-1/2)\nu_o t} \quad . \tag{2.18}$$

This is the output in response to a monochromatic input having for frequency any odd integral multiple of half the sampling frequency. If the function $W(\nu)$ is represented by a contour on the complex plane (e.g., Fig. 2.10), each of the interference terms in the output (Eqs. 2.16, 2.17, 2.18) adds a circle centered on $W\left[(k-1/2)\nu_o\right]$ and passing through the origin.

2.4.2. <u>Behavior at multiples of sampling frequency.</u> The behavior described above also occurs at any integral multiple of sampling frequency. To show this one takes Eq. (2.7), and without rearranging, lets $\nu = \delta\nu$, $\delta\nu/\nu_o << 1$ as before, realizing that, as previously, in the limit $W(n\nu_o \pm \delta\nu)$ approaches $W(n\nu_o)$ as $\delta\nu$ is allowed to vanish. Thus the factors $W(n\nu_o)\exp(2\pi i n\nu_o t)$ are removed. Again, as before, phase is referred in each term to the lower frequency spectrum line. Thus we have the set of equations

$$F_n(t)\exp\left[-2\pi i(n\nu_o-\delta\nu)t\right] = \frac{a}{2}\, W(n\nu_o)\left[1+e^{4\pi i\delta\nu t}\right] \tag{2.19}$$

All the remarks made with reference to the $\nu_o/2$ case apply here. This case, however, is trivial in the clamped sampler, since $W(n\nu_o) = 0$ for all n. For samplers having pulse shapes other than square, $W(n\nu_o)$ does not in general vanish, and one thus finds interference at all integral multiples of half the sampling frequency.

2.4.3. Particularization to the clamped sampler. A case in point is the clamped sampler, the pulse shape being square, and of length $1/\nu_o$, whence

$$W\left[(k-1/2)\nu_o\right] = -i \frac{2}{(2k-1)\pi} \tag{2.20}$$

and so

$$F(t) = -i \frac{a}{2} \frac{2}{\pi} (1+e^{2i\phi}) \sum_{k=-\infty}^{\infty} \frac{e^{2\pi i(k-1/2)\nu_o t}}{2k-1} \tag{2.21}$$

This case is illustrated in Fig. 2.11. The first order shows the largest and most important effect in the clamped case, and hence is given special attention in Fig. 2.12. Using the clamped sampler as an illustration of the general case, and taking the perturbation once more, we have the input-frequency component arbitrarily close to $\nu_o/2$, and the difference frequency component symmetrically disposed beyond $\nu_o/2$. The latter case precesses in phase about the 'fundamental', or input-frequency component, at a rate equal, in precession periods per second, to the separation $(2\delta\nu)$ between the two spectrum lines. If at any time we remove the perturbation, we have a possible combination of circumstances in the limit at $\nu_o/2$. Thus, solely due to chance, the output phase at $\nu_o/2$ could lie anywhere on the circular locus shown. The accidental nature of this interference phenomenon of course makes the transfer function discontinuous at $(2n-1)\nu_o/2$, with the transfer function consisting of $W(\nu_o)$ plus the set of circles discussed above.

2.4.4. Particularization to the impulse case. The case where the sampling pulses are unit impulses is of interest, as it has been used in the work of both Linvill and Bennett. While the results of Sections 2.3.1 and 2.3.2 are perfectly general, and indicate the result, some explicit remarks may be in order here.

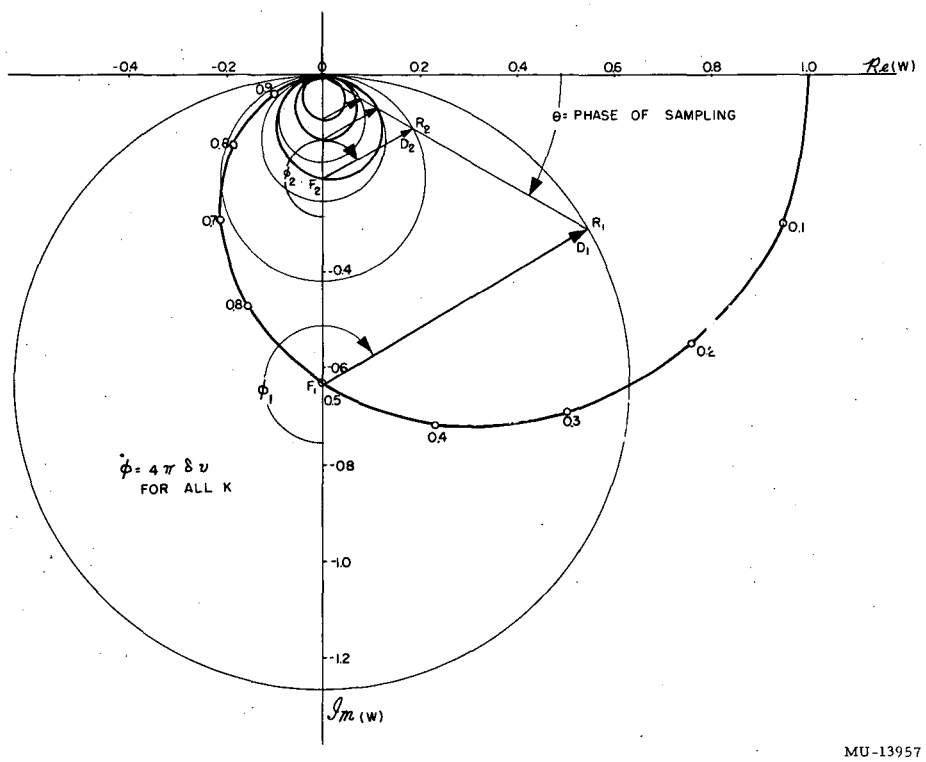

Fig. 2.11. Complete transfer function for the clamped sampler in the first four orders, with the interference structure occurring at n $\nu_o/2$ shown.

F_k are sum-frequency components of kth order.

D_k are difference-frequency components.

R_k are the resultants.

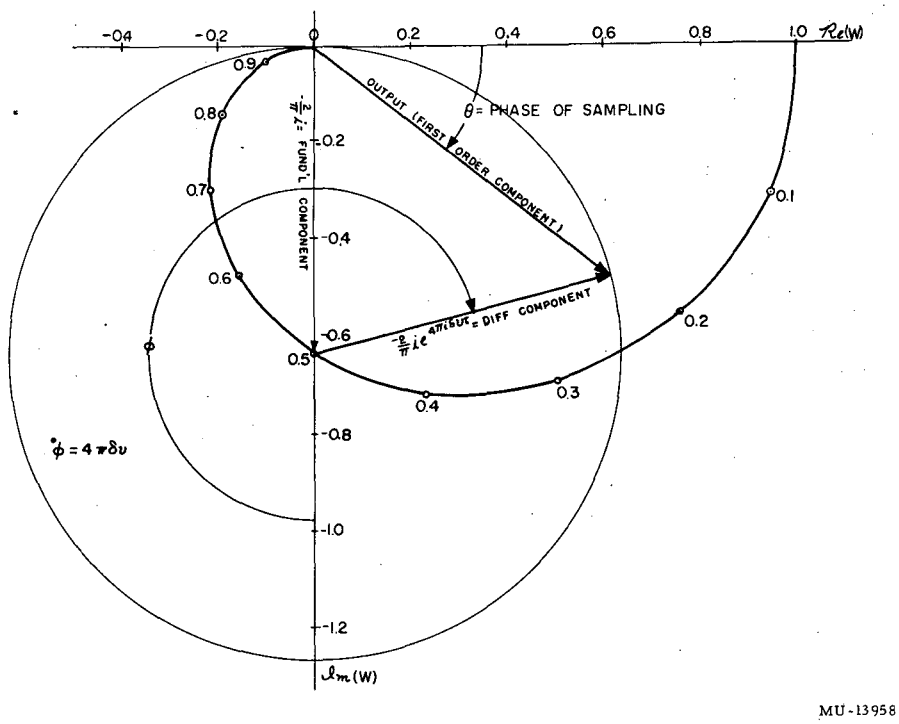

Fig. 2.12. Region below the first zero of the sampler transfer function of Fig. 2.11, showing mechanism of interference between spectral components of sampler output at half-sampling frequency.

Let now the pulse shape be

$$g(t) = \delta(t) \tag{2.22}$$

$\delta(t)$ being the Dirac δ-function,

$$\delta(t) = \lim_{a \to 0} S(t, a) \tag{2.23}$$

$$S(t, a) = \frac{1}{\sqrt{2\pi}} \frac{1}{a} e^{-\frac{t^2}{2a^2}} \tag{2.24}$$

$S(t, a)$ is a Gaussian of width a and amplitude $1/a$, so that

$$\int_{-\infty}^{\infty} S(t, a)\, dt = 1 \quad \text{for all} \quad a.$$

Substituting the above into Eq. (2.4) and performing the integration,

$$W(\nu) = \lim_{a \to 0} W(\nu, a) \tag{2.25}$$

$$W(\nu, a) = e^{-2\pi^2 a^2 \nu^2} \tag{2.26}$$

Combined, Eqs. (2.16) and (2.19) are

$$F_n(t) \exp\left[-2\pi i \left(m \frac{\nu_o}{2} - \delta\nu\right)t\right] = W\left(m \frac{\nu_o}{2}\right)\left[1 + e^{4\pi i \delta\nu t}\right]$$

For $W(m \frac{\nu_o}{2})$ we substitute the expression of (2.26), with $\nu = \nu_o/2$, and pass to the limit $a = 0$:

$$F_n(t) \exp\left[-2\pi i \left(m \frac{\nu_o}{2} - \delta\nu\right)t\right] = 1 + e^{2\pi i (2\delta\nu)t} \tag{2.27}$$

All orders have their interference circles superposed in a single one centered on the point $1 + 0i$.

To consider the sampling-function to occur on an impulse basis in any physical system is of course a mathematical idealization. One can profitably make this idealization if the actual pulse shape can be attributed to linear passive networks, since the function of these can be readily described in terms of a transfer function. If, however, the pulse shaping is due to the

action of nonlinear, and/or active networks, things are not so simple, and usually the approach of the present work, namely, describing the transfer properties of a physical sampler in terms of its pulse shape, has the advantage of simplicity and realism. In any event, the δ-function idealization does not in any respect whatever free one from the interference phenomenon. It is an essential result of the quantization of time, and of nothing else.

One might also note that the impulse-sampler is only a moderate idealization of a physical one using short pulses, and illustrates one significant feature of the latter: the shorter the sampling pulse, the smaller the output amplitude, for a given input. In fact, the output-to-input amplitude ratio is proportional to the pulse-width, a, for the Gaussian shape, which comes fairly close to being representative of very short electronically-generated pulses.

2.5. Sampler output corresponding to an arbitrary periodic input of period near $2/\nu_o$. To facilitate discussion in the next chapter, of the stability question, this section will treat the matter of the output resulting from an arbitrary periodic input whose period is close to twice the sampling period. To start with, the input and output are given by Eqs. (2.1) and (2.3), respectively, with only one value of S:

$$f(t) = \sum_{m=-\infty}^{\infty} c_m e^{im\omega t}$$

and

$$F(t) = \sum_{m=-\infty}^{\infty} \sum_{n=-\infty}^{\infty} c_m W(n\omega_o + m\omega)\, e^{i(n\omega_o + m\omega)t}$$

which can be written

$$F(t) = \sum_{n=-\infty}^{\infty} c_o W(n\omega_o)\, e^{in\omega_o t} + \sum_{m=1}^{\infty} \sum_{n=-\infty}^{\infty} \Big[c_m W(n\omega_o + m\omega)\, e^{i(n\omega_o + m\omega)t} + c_{-m} W(n\omega_o - m\omega)\, e^{i(n\omega_o - m\omega)t} \Big]. \qquad (2.28)$$

For convenience, we call the double-sum term by the name H(t). Now we apply Eq. (2.13):

$$H(t) = \sum_{m=1}^{\infty} \sum_{n=-\infty}^{\infty} \left\{ c_m W(n\omega_o + m \frac{\omega_o}{2} - m\delta\omega)\, e^{i(n\omega_o + m\frac{\omega_o}{2} - m\delta\omega)t} + c_{-m} W(n\omega_o - m\frac{\omega_o}{2} + m\delta\omega)\, e^{i(n\omega_o - m\frac{\omega_o}{2} + m\delta\omega)t} \right\} \tag{2.29}$$

In (2.29) we wish to shift the order of summation so as to pair off terms whose frequency arguments are separated only by $\delta\omega$, making the explicit provision that the analysis will apply only to pulse shapes such that

$$W(\omega \pm \delta\omega) = W(\omega), \quad \delta\omega << \omega \tag{2.30}$$

i.e., that the function $W(\omega)$ is analytic (it can be shown that a convergent Fourier transform is an analytic function). In order to carry this off we imagine the second n-sum (that involving c_{-m}) in Eq. (2.29) to have an index k instead of n; then what we wish to impose is the condition

$$n\omega_o + m\frac{\omega_o}{2} = k\omega_o - m\frac{\omega_o}{2}$$

or

$$n + m = k \tag{2.31}$$

Equation (2.31), solved for n, is substituted into the first n-sum of Eq. (2.29), and the whole business is now summed on the index k, resulting in

$$H(t) = \sum_{m=1}^{\infty} \sum_{k=-\infty}^{\infty} \left\{ c_m W\left[(2k-m)\frac{\omega_o}{2} - m\delta\omega\right] e^{i\left[(2k-m)\frac{\omega_o}{2} - m\delta\omega\right]t} + c_{-m} W\left[(2k-m)\frac{\omega_o}{2} + m\delta\omega\right] e^{i\left[(2k-m)\frac{\omega_o}{2} + m\delta\omega\right]t} \right\} \tag{2.32}$$

In light of Eq. (2.30), for sufficiently small $\delta\omega/\omega$,

$$H(t) = \sum_{m=1}^{\infty} \sum_{k=-\infty}^{\infty} c_m W\left[(2k-m)\frac{\omega_o}{2}\right] e^{i\left[(2k-m)\frac{\omega_o}{2} - m\delta\omega\right]t} \cdot \left[1 + \frac{c_{-m}}{c_m} e^{2im\delta\omega t}\right] \tag{2.33}$$

The quantity $2\delta\omega t$ is the precession rate of the sampling instant. If the perturbation is removed the process is stopped ('frozen') at some particular value of sampling phase, reckoned on the scale $2\pi = 2/\nu_o$ (phase referred to the fundamental frequency component of the spectrum). Thus we call

$$t\delta\omega = \phi(t) \tag{2.34}$$

the sampling phase, whose zero is reckoned from the maximum value of the exponential, i.e., from the time of reinforcement (were c_m and c_{-m} to be real).

Referring to the expression for $f(t)$, one sees that in order that $f(t)$ be real,

$$c_m = c_{-m}^* \quad \text{(complex conjugate)} \tag{2.35}$$

thus,

$$c_m = \mathscr{b}_m e^{i\theta_m} \tag{2.36a}$$

$$c_{-m} = \mathscr{b}_m e^{-i\theta_m} \tag{2.36b}$$

so

$$\frac{c_{-m}}{c_m} = e^{-2i\theta_m}$$

and the last (bracketed) factor in Eq. (2.33) becomes

$$1 + e^{2i(m\phi - \theta_m)}$$

Particular interest lies in the case where input frequency is precisely $\nu_o/2$; eq. (2.33) is, with the perturbation removed (and with slight rearrangement),

$$H(t) = \sum_{m=1}^{\infty} c_m \left[1 + e^{2i(m\phi - \theta_m)}\right] \sum_{k=-\infty}^{\infty} W\left[(k - \frac{m}{2})\omega_o\right] e^{i(k-\frac{m}{2})\omega_o t} \tag{2.37}$$

The entire output is

$$F(t) = \sum_{k=-\infty}^{\infty} c_o W(k\omega_o)\, e^{ik\omega_o t} + H(t) \qquad (2.38)$$

As noted above, θ_m is the phase of c_m, and ϕ is the phase of sampling. With regard to this latter item, some remarks may be pertinent, as there is considerable potential for ambiguity at this point.

In the case $m = 1$ (the so-called 'fundamental' component of the input spectrum) the argument of the interference term is $2i(\theta_1 - \phi)$, giving maximum value to the term at $\phi = \theta_1$. Likewise, for each order, the term reaches its maximum value when $m\phi = \theta_m$. Now ϕ is the phase of the 'fundamental', or first-order term at which sampling occurs, give or take some constant depending upon input waveform; the zero of ϕ, is determined by the fact that maximum first-order output obtains if sampling occurs at $\phi = \theta_1$, the phase of any component being, of course, referred back to the interval between successive occurrences of any particular value of the input time-function (i.e., the interval over which the Fourier coefficients are integrated).

In Eq. (2.38), the first series represents the output corresponding to the average value, or zero-order term, of the input, and consists of a track of identical pulses; superposed upon this is the dynamic output signal, H(t), of Eq. (2.37).

The function H(t) (Eq. 2.37) is to be compared with the function F(t) of Eq. (2.18). In (2.37), each term of the sum on m consists of, firstly, the Fourier coefficient of the input component of mth order; secondly, the mth order interference factor $1 + \exp(2i\psi_m)$, where $\psi_m = m\phi - \theta_m$, is the phase at which the mth order component is sampled. Thirdly, there is the output pulse-train, embodied in the k-sum (note that the index m enters here, too, so that Eq. (2.37) is not the product of two series, but is a double Fourier series. The (partial) argument $(m/2)\,\omega_o$ is the frequency of the mth order spectrum line of the input, and output. The complete argument $(k-m/2)\omega_o$ is the set of frequencies of the set of spectrum lines resulting from the mth order input component.

It is profitable to write H(t) in another way; since the argument of the k-series in Eq. (2.37) may be written $(2k-m)\,\omega_o/2$, and since the factor

(2k-m) is a dummy variable, it may be used as the index of summation. It is dependent upon m only in the matter of odd-ness or even-ness, i.e., if m is odd, (2k-m) is odd; if m is even, (2k-m) is even. Thus it is possible to break up H(t) into two double sums, one involving only even values both of indices m and k, the other involving only odd values of both indices. At this juncture it becomes apparent that each sum, odd and even, is the product of two series, which can be rearranged to render the output

$$F(t) = \sum_{k=-\infty}^{\infty} \left\{ \left[c_o + \sum_{m=1}^{\infty} c_{2m} (1 + e^{2i(2m\phi - \theta_{2m})}) \right] W(2k \frac{\omega_o}{2}) \, e^{2ik \frac{\omega_o}{2} t} \right.$$

$$+ \sum_{m=1}^{\infty} c_{2m-1} (1 + e^{2i\left[(2m-1)\phi - \theta_{2m-1}\right]})$$

$$\left. W\left[(2k-1) \frac{\omega_o}{2}\right] e^{i(2k-1)\frac{\omega_o}{2} t} \right\} \tag{2.39}$$

It is instructive to compare Eqs. (2.39) and (2.18). In the case of a monochromatic input of period $2/\nu_o$, a symmetrical output is generated. However, when the input is not symmetrical, albeit of period $2/\nu_o$, the output cannot be symmetrical unless (and only unless) the sampling instants happen to fall at equal positive and negative values of the input. Such an event would be fortuitous indeed. In general, a nonsymmetrical periodic input generates an output in which the even-order spectrum lines are quite as important as those of odd order.

As an informative application consider the input to be

$$f(t) = \sum_{m=-\infty}^{\infty} c_m e^{im\omega t} = a\,(1 + \cos \frac{\omega_o}{2} t).$$

Here $c_o = a$, $c_{-1} = c_1 = \frac{a}{2}$, $c_m = 0$ for all $m \neq -1, 0,$ or $+1$; $\theta_m = 0$ for all m. In Eq. (2.8), let $\nu_1 = 0$, $\nu_2 = \frac{\nu_o}{2}$. There results an equation for F(t) which is the sum of sampler outputs corresponding to (1) the dc component of the input (above), (2) its sinusoidal part. Using

the results of Section 2.4.1 we have the latter output expressed precisely in Eq. (2.18). Substituting the above values for the c_m and the θ_m in Eq. (2.39), we arrive at precisely the same result.

3. THE PROBLEM OF STABILITY IN A FEEDBACK LOOP

In an ordinary (continuous control) feedback system, the criterion of Nyquist applies to the frequency transfer-function of the entire loop, i.e., to the transfer-function which operates upon signals passing around the loop.

One must hold certain reservations when he uses the term 'transfer function' in connection with a sampler, as the sampler is an essentially nonlinear device. What we have called the 'transfer function' of a sampler certainly cannot be combined with those of a sequence of linear elements in the usual manner and directly subjected to Nyquist's criterion; this 'transfer function' for the whole loop, so derived, however, can be used to generate a function having properties similar to those of the true transfer-function for a series of cascaded linear networks. This function is characteristic of the particular time-quantized feedback loop under con-consideration, and to it the stability criterion of Nyquist can be directly applied as for a completely linear system.

This extended Nyquist criterion is developed by Linvill[3] and by Ragazzini and Zadeh.[5] These authors do not, however, explicity recongnize the 'sampling oscillations' which occur with a period of $\nu_o/2$. Linvill seems in fact to attribute such oscillations to nonlinearities in the output member of the system ('saturation effects'); the trouble, rather, arises in the sampler itself, and solely from the sampling process. Lago and Truxal[6] recognize sampling-oscillations, and insist that the extended Nyquist criterion applies.

The authors have felt certain doubts as to whether the extended criterion as so far put forth fully accounts for all of the troubles at half-sampling frequency. Therefore, in the section to follow there is a somewhat lengthy, but general, demonstration of the fact that it does. In a later section there is a derivation of the extended criterion from the point of view adopted with reference to sampling oscillations, and the criterion is stated in a manner readily interpretable from a physical (geometrical)

---

[3] Linvill, op. cit.

[5] Ragazzini and Zadeh, op. cit.

[6] Lago and Truxal, op. cit.

standpoint, lending itself to a geometrical method for estimation of critical gain in practical applications. These interpretations are subsequently developed.

3.1 Conditions for the occurrence of oscillations having a period of $2/\nu_o$.

One might be inclined to think that Nyquist's criterion might be extended to the time-quantized situation by mere inclusion of the interference circles as parts of the transfer function; certainly they are, but it is not enough to state that self-sustaining oscillations will occur if a circle encloses the critical point. In some cases a system with sampling will oscillate at values of gain materially lower than that required to cause enclosure of the critical point; in others, enclosure occurs without ill effects. Such oscillations would occur only at half the sampling frequency, for an oscillation at any odd multiple of $\nu_o/2$ will be reduced to frequency $\nu_o/2$ by the sampling process, itself, and any signal whatever having for a frequency any integral multiple of sampling frequency itself will be reduced by the sampling process to a train of identical (sampling) pulses.

The term "oscillation 'at' half-sampling frequency" connotes a looseness of usage which will for present purposes be convenient. It means just this: that the output waveform (of the sampler) consists of a train of like pulses which are alternately positive and negative in polarity, i.e., for a clamped sampler, the output is a 'square-wave'. Thus the terminology is correct in this sense: that the output waveform is that associated with a monochromatic input of frequency $\nu_o/2$, and of course, the input is a periodic function having period $2/\nu_o$, with waveform which depends upon the sampler pulse shape and upon the transfer properties of the remainder of the loop.

Existence of oscillations in general at a gain level other than that required to cause enclosure of the critical point by an interference circle is due to the waveform effect, or to put it another way, to the cumulative interferences in all of the various orders. Thus, the gain required to produce these oscillations is dependent upon the transfer function $W(\nu)$, and upon the loop transfer properties, since these literally determine how many orders are important contributors to the oscillation.

The time has now come for the derivation of a quantitative condition for the stability of a feedback loop with reference to oscillations of period $2/\nu_o$. Consider a feedback loop from the point of view of Fig. 3.1.

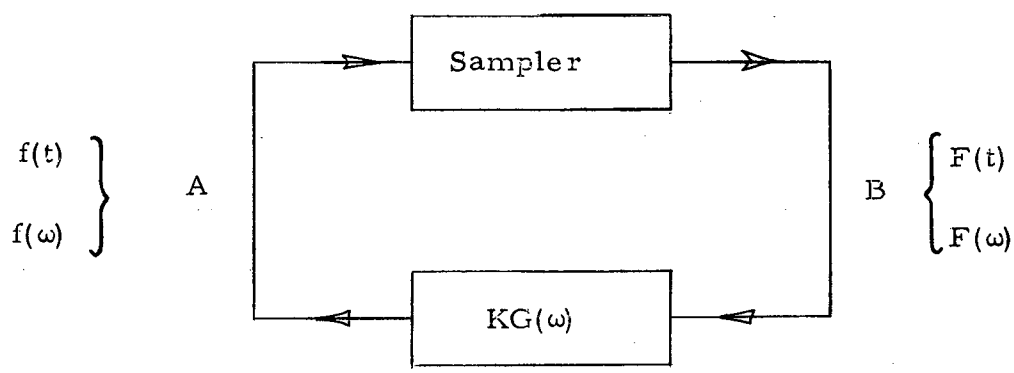

Fig. 3.1. Feedback loop containing a sampler and elements whose transfer properties can be described by the function $KG(\omega)$. K is the returnpath gain; $G(\omega)$ is its frequency characteristic.

At A, the sampler input is f(t), having a spectrum $f(\omega)$, a line spectrum, whose line of lowest frequency is at $\nu_o/2$. At B, the sampler output is F(t), spectrum $F(\omega)$, also a line spectrum. It will be assumed that the loop is in a barely oscillating condition, hence the signals at A and B are related by the oscillation condition

$$f(\omega) = - KG(\omega)\, F(\omega) \tag{3.1}$$

where f and F are corresponding sampler input and output, in the notation of section 2.2. Now (3.1) represents the operation of $-KG(\omega)$ on each spectrum line (Fourier coefficient) of F(t), and implies that f(t) is the recombination of the resulting spectrum in a time function expressed by a Fourier series; thus, if

$$F(t) = \sum_{m=-\infty}^{\infty} \lambda_m e^{im \frac{\omega_o}{2} t} \tag{3.2}$$

$$f(t) = \sum_{m=-\infty}^{\infty} c_m e^{im \frac{\omega_o}{2} t} \tag{3.3}$$

hence

$$c_m = - KG(m \frac{\omega_o}{2}) \lambda_m \tag{3.4}$$

The λ_m can be determined from Eq. (2.39), which describes the sampler output corresponding to an arbitrarily shaped periodic input having twice the sampling period. There are certain observations, however, which can be made regarding the possible nature of the oscillations, and which can save much labor in the calculations. To start with, a zero-frequency component will not circulate around the loop, since feedback is by definition 'inverse' to frequencies near zero. Furthermore, were the waveform unsymmetrical, it would possess components having frequencies which were even-integer multiples of half the sampling frequency, and vice versa. It has been shown, however, that insofar as the results of the sampling process are concerned, any input having sampling frequency or any integral multiple thereof is tantamount to a "dc" input, which due to the action of the feedback process, would be suppressed. Thus only a symmetrical oscillation can exist in the steady state, and therefore can contain only components whose frequencies are odd-integer multiples of $\nu_o/2$.

Thus, the most general form of the sampler output F(t) under the oscillation condition is given by the sum of the odd-order terms in Eq. (2.39), wherein the notation with respect to the summation indices k and m will be interchanged for the sake of convenience. The resulting expression is

$$F(t) = \sum_{m=-\infty}^{\infty} \sum_{k=1}^{\infty} c_{2k-1} \left[1 + e^{2i\left[(2k-1)\phi - \theta_{2k-1}\right]}\right] W\left[(2m-1)\frac{\omega_o}{2}\right] e^{i(2m-1)\frac{\omega_o}{2} t} \tag{3.5}$$

Thus by comparing Eqs. (3.2) and (3.5) we have the expressions for the λ_m:

$$\lambda_{2m} = c_{2m} = 0 \tag{3.6a}$$

$$\lambda_{2m-1} = \sum_{k=1}^{\infty} c_{2k-1} \left(1 + e^{2i\left[(2k-1)\phi - \theta_{2k-1}\right]}\right) W\left[(2m-1)\frac{\omega_o}{2}\right] \tag{3.6b}$$

Then, from Eq. (3.4),

$$c_{2m-1} = -K \sum_{n=1}^{\infty} c_{2n-1}\left(1 + e^{2i\left[(2n-1)\phi - \theta_{2n-1}\right]}\right) W\left[(2m-1)\frac{\omega_o}{2}\right] G\left[(2m-1)\frac{\omega_o}{2}\right] \tag{3.7}$$

Now Eq. (3.5) gives F(t) in terms of input waveform parameters and sampling phase. One can also write it in terms of sampler pulse shape and an arbitrary amplitude coefficient, then apply Eq. (3.4) to get a relation between the c_m and c_{-m}; this is because the output waveform corresponding to an arbitrary, symmetrical, input of period $2/\nu_o$ is the same as that corresponding to some sinusoidal input whose amplitude depends somehow upon sampling phase and waveform. Thus, we use Eq. (2.7), with $\omega = \frac{\omega_o}{2}$ which when simplified becomes

$$F(t) = a \sum_{m=-\infty}^{\infty} W\left[(2m-1)\frac{\omega_o}{2}\right] e^{i(2m-1)\frac{\omega_o}{2}t} \tag{3.8}$$

the coefficient a now being a function of ϕ and the θ_{2m-1}.

Now a value of a may be found to make Eq. (3.8) identical with Eq. (3.5) for any waveform of the type under discussion. From (3.8), compared with (3.2),

$$\lambda_{2m-1} = a \quad W\left[(2m-1)\frac{\omega_o}{2}\right] \tag{3.9}$$

and hence from (3.4),

$$c_{2m-1} = -a \quad KG\left[(2m-1)\frac{\omega_o}{2}\right] \quad W\left[(2m-1)\frac{\omega_o}{2}\right] \tag{3.10}$$

Equating either (3.9) to (3.6b) or (3.10) to (3.7) gives

$$a = \sum_{k=1}^{\infty} c_{2k-1} \left(1 + e^{2i\left[(2k-1)\phi - \theta_{2k-1}\right]}\right) \tag{3.11}$$

Now we multiply Eq. (3.10) by $\left(1 + e^{2i\left[(2m-1)\phi - \theta_{2m-1}\right]}\right)$ and sum on m; the member on the left, by Eq. (3.11), is precisely a, yielding

$$-\frac{1}{K} = \sum_{m=1}^{\infty} \left(1 + e^{2i\left[(2m-1)\phi - \theta_{2m-1}\right]}\right) G\left[(2m-1)\frac{\omega_o}{2}\right] W\left[(2m-1)\frac{\omega_o}{2}\right]. \tag{3.12}$$

Now the θ_{2m-1} are the phases of the Fourier coefficients of the sampler input. Thus, using Eq. (3.10) once more,

$$e^{-2i\theta_{2m-1}} = \frac{c_{-(2m-1)}}{c_{2m-1}}$$

$$= \frac{G\left(-\left[2m-1\right]\frac{\omega_o}{2}\right) W\left(-\left[2m-1\right]\frac{\omega_o}{2}\right.}{G\left(\left[2m-1\right]\frac{\omega_o}{2}\right) W\left(\left[2m-1\right]\frac{\omega_o}{2}\right)} \tag{3.13}$$

In order for $G(\omega)$ to be the transfer function of a physically realizable network,[12] $G(-\omega) = G^*(\omega)$; moreover, from Eq. (2.4), $W(-\omega) = W^*(\omega)$, where the asterisk (*) denotes the complex conjugate. It appears then, that

$$\theta_{2m-1} = \arg G\left(\left[2m-1\right]\frac{\omega_o}{2}\right) + \arg W\left(\left[2m-1\right]\frac{\omega_o}{2}\right). \tag{3.14}$$

Equation (3.12) is the condition for oscillation; it is necessary, however, to separate it into real and imaginary parts, for which purpose Eq. (3.13) can be helpful, when substituted in Eq. (3.12):

[12] Bode, H. W., Network Analysis and Feedback Amplifier Design, Sec. 7.3, pp. 106 ff., Van Nostrand (1945).

$$-\frac{1}{K} = \sum_{m=1}^{\infty}\left\{G\left(\left[2m-1\right]\frac{\omega_o}{2}\right) W\left(\left[2m-1\right]\frac{\omega_o}{2}\right.\right.$$

$$\left.\left. + e^{2i(2m-1)\phi} G\left(-\left[2m-1\right]\frac{\omega_o}{2}\right) W\left(-\left[2m-1\right]\frac{\omega_o}{2}\right)\right\}$$

(3.15)

Now each of the functions G and W is a complex function of the single real variable, ω. Thus, letting X, Y, U, and V be real, even functions of ω,

$$G(\pm\omega) = X(\omega) \pm iY(\omega) \tag{3.16a}$$

$$W(\pm\omega) = U(\omega) \pm iV(\omega) \tag{3.16b}$$

whence the real part of Eq. (3.15) is

$$\sum_{m=1}^{\infty}\left\{\left[X_m U_m - Y_m V_m\right]\left[1 + \cos 2(2m-1)\phi\right] + \sin 2(2m-1)\phi\left[X_m V_m + Y_m U_m\right]\right\} = -\frac{1}{K}$$

(3.17)

and the imaginary part is

$$\sum_{m=1}^{\infty}\left[X_m V_m + Y_m U_m\right]\left[1 - \cos 2(2m-1)\phi\right] + \sin 2(2m-1)\phi\left[X_m U_m - Y_m V_m\right] = 0$$

(3.18)

in which the subscript m indicates evaluation of the function at $\omega = (2m-1)\frac{\omega_o}{2}$. Equation (3.18) is satisfied by $\phi = n\pi$, n being zero or a positive integer. If one looks momentarily at the oscillation process as a repetitive transient phenomenon, it is readily apparent that the phase of sampling, in the oscillation waveform, is an invariant of the system, as is the waveform at the sampler input. The sampling phase is fixed; it cannot differ. For suppose that somehow sampling were to occur at a 'different' phase; then the transient response to the sampling pulse would occur as before (i.e., the sampler output

pulse would be modified in the same way as before), the only possibly excepted aspect being amplitude of the waveform. Sampling would occur after the usual interval $(1/\nu_o)$, and the same identical transient (modified sampling pulse shape) would have occurred in the interim. Therefore sampling phase was not 'different' after all. We are perfectly at liberty to reckon the zero of phase from this point of the waveform; indeed, Eq. (3.18) dictates this turn of events. Phase of sampling is therefore taken as zero. In light of the foregoing, Eq. (3.17) reduces immediately to

$$\sum_{m=1}^{\infty} 2(X_m U_m - Y_m V_m) = - \frac{1}{K} \tag{3.19}$$

This is the criterion for stability which applies to oscillation at half the sampling frequency, and which extends the criterion of Nyquist to the time-quantized feedback system.

The criterion of Eq. (3.19) has a simple and direct physical interpreation. The (normalized) loop transfer function, one recalls, is $G(\omega)W(\omega)$; referring to Eqs. (3.16a) and (3.16b) it is readily seen that Eq. (3.19) is precisely

$$\sum_{m=1}^{\infty} 2\mathrm{Re}\left\{G(\omega_m)W(\omega_m)\right\} = - \frac{1}{K} \tag{3.20}$$

Thus, the cumulative algebraic sum of the real-axis intercepts of the interference circles must not reach the point $(1/K) - 0i$, or sampling-oscillations will occur. The geometrical situation is shown in Fig. 3.2. It is to be noted that in the case chosen for Fig. 3.2, the sampling-oscillations could not occur, since the loop gain must be a positive quantity, and since the sum of Eq. (3.20) is itself positive. Hence the oscillation-condition can never be reached. This answers the question as to whether oscillation must occur if some interference-circle loops about the critical point. The answer is a resounding 'no', since the waveform at sampler input is made up of the <u>sum</u> of contributions from all the orders; even though were one of these by itself large enough to encircle the critical point, its effects will be modified by the cumulative sum of the contributions from all of the other orders. It is the resultant effect alone which can cause oscillations.

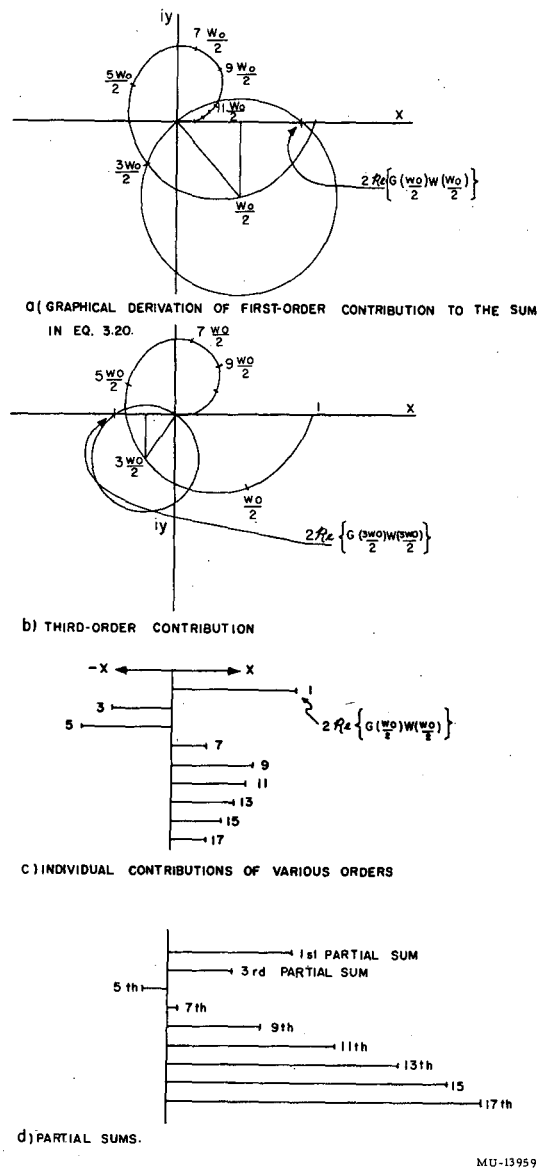

Fig. 3.2. Geometrical interpretation of the stability criterion of Eq. (3.20) for a hypothetical feedback loop, having a frequency characteristic $G(\omega)\ W(\omega)$. Note (from d) that this hypothetical system could not possibly undergo sampling oscillations.

3.2. Application to the clamped, and impulse cases. In the case of clamped sampling the application of Eq. (3.19) is made by recourse to Eq. (2.20), which in (3.16b) gives

$$U_m \equiv 0$$

$$V_m = -\frac{2}{\pi}\frac{1}{2m-1}$$

So Eq. (3.19) becomes (using the more customary notation in place of the subscripts)

$$\frac{4}{\pi}\sum_{m=1}^{\infty}\frac{1}{2m-1}\,Y\left(\left[2m-1\right]\frac{\omega_o}{2}\right) = -\frac{1}{K} \tag{3.21}$$

Y being defined in Eq. (3.16a) as the imaginary part of the (normalized) loop frequency characteristic, K being the 'loop gain' (normalizing constant).

The impulse-sampler is quite different; here

$$W(\nu) = 1$$

hence

$$U_m = 1$$

$$V_m \equiv 0$$

and Eq. (3.19) is

$$\sum_{m=1}^{\infty} 2X\left(\left[2m-1\right]\frac{\omega_o}{2}\right) = -\frac{1}{K} \tag{3.22}$$

standing in interesting contrast to the clamped case.

3.3 General case of feedback oscillations. The oscillation condition for the general case proves easier to derive than that for oscillations of period $2/\nu_o$. Once again, we refer to Fig. 3.1, and to Eq. (3.1), wherein ω is no longer considered to be necessarily related to $\omega_o/2$. The loop is considered to be closed at A, where in the oscillating condition the input equals the output, with reversed sign (the feedback, by definition, is 'inverse' for low frequencies). Thus regeneration occurs, as postulated.

Since the oscillation (in order to be an oscillation) is periodic, Eqs. (2.1) and (2.3) hold with all the $c_{ms} = 0$ excepting the set $c_{m1} = c_m$. Thus, these equations are written, assuming an oscillation having a period $2\pi/\omega$

$$f(t) = \sum_{m=-\infty}^{\infty} c_m e^{im\omega t} \tag{3.23}$$

$$F(t) = \sum_{m=-\infty}^{\infty} \sum_{n=-\infty}^{\infty} c_m W(n\omega_o + m\omega) e^{i(n\omega_o + m\omega)t} \tag{3.24}$$

Since $F(t)$ and $f(t)$ are both real, $c_{-m} = c_m$ and $W(-\omega) = W^*(\omega)$.

Now there are precisely as many lines in the spectrum of $f(t)$ as there are in that of $F(t)$. And to every line of F applies the condition of Eq. (3.1) to make up the corresponding line in f; thus,

$$f(t) = -K \sum_{m=-\infty}^{\infty} \sum_{n=-\infty}^{\infty} c_m GW(n\omega_o + m\omega) e^{i(n\omega_o + m\omega)t} \tag{3.25}$$

where we will mean by the notation

$$GW(n\omega_o + m\omega) \equiv G(n\omega_o + m\omega)\ W(n\omega_o + m\omega). \tag{3.26}$$

Following Linvill, we trace the line of frequency ω: in the sampling process (transition from $f(t)$ to $F(t)$),

$$c_o e^{i\omega t} \quad \text{becomes} \quad c_o W(\omega) e^{i\omega t} \quad \text{plus other terms.} \tag{3.27}$$

Likewise, every component of $f(t)$ having a frequency in the set $(n\omega_o + \omega)$ will contribute a line of frequency ω in F as it passes through the sampler. Since these all arose from the $m = 0$ term (frequency ω), they have the coefficient c_o; thus

$$-K\, c_o\, GW(n\omega_o + \omega)\ e^{i(n\omega_o + \omega)t} \quad \text{becomes}$$

$$-K\, c_o\, GW(n\omega_o + \omega)\ W(\omega)\ e^{i\omega t} \quad \text{plus other terms.} \tag{3.28}$$

The total amplitude of the term of frequency ω will be the sum of all of the contributions, to wit

$$- K c_o W(\omega) e^{i\omega t} \sum_{n=-\infty}^{\infty} GW(n\omega_o + \omega) \tag{3.29}$$

This is the term of frequency ω in $F(t)$; equating this to the term value in (3.27) yields the oscillation condition for the (arbitrary) frequency ω:

$$1 + K \sum_{n=-\infty}^{\infty} GW(n\omega_o + \omega) = 0 \tag{3.30}$$

The left-hand member of (3.30) is the denominator of Linvill's Eq. (15)[3] and is the stability-determining factor in all of Ragazzini and Zadeh's single-sampler systems listed in their Table II.[5]

Equation (3.30) is the general oscillation-condition; to the function

$$K \sum_{n=-\infty}^{\infty} GW(n\omega_o + \omega) \tag{3.31}$$

the criterion of Nyquist is applied in the customary manner. As will be presently seen, Eq. (3.30) includes Eq. (3.20) as a special case. Out of that demonstration will, moreover, come some interesting results regarding properties of expression (3.31).

The sum in expression (3.31) is

$$S(\omega) = GW(\omega) + \sum_{n=1}^{\infty} GW(n\omega_o + \omega) + GW(-n\omega_o + \omega)$$

Now

$(-n\omega_o + \omega) = -(n\omega_o - \omega)$, and in light of Eqs. (3.16), $GW(-n\omega_o + \omega) = G^* W^*(-[n\omega_o - \omega]) = \overline{GW}^*(-[n\omega_o - \omega])$, so

$$S(\omega) = GW(\omega) + \sum_{n=1}^{\infty} \left[GW(n\omega_o + \omega) + \overline{GW}^*(n\omega_o - \omega)\right] \tag{3.32}$$

---

[3] Linvill, op. cot.

[5] Ragazzini and Zadeh, op. cit.

which is a complex function of the real variable, ω. Let, now $\omega = \omega_o/2$; then, in (3.32) the argument of the first term is $\omega_o/2$, that of the first term in the bracket is $(2n + 1)\,\omega_o/2$, and in the second bracketed term, $(2n-1)\,\omega_o/2$. Considering the bracket as two separate sums, now, the leading term of the second has argument $\omega_o/2$, with second term (n=2) having the argument $3\,\omega_o/2$, as has the leading term of the first sum. Since n is a dummy variable, the argument of the general term in the first sum may be made $(2n-1)\,\omega_o/2$ and the summation range changed from n = 2 to ∞; thus, all the terms in Eq. (3.32) combine to give

$$S\left(\frac{\omega_o}{2}\right) = \sum_{n=1}^{\infty} \left[GW\left(\left[2n-1\right]\frac{\omega_o}{2}\right) + \overline{GW}^{*}\left(\left[2n-1\right]\frac{\omega_o}{2}\right)\right]$$

which is nothing more than

$$S = \sum_{n=1}^{\infty} 2\mathrm{Re}\, GW\left(\left[2n-1\right]\frac{\omega_o}{2}\right) \tag{3.33}$$

Thus, $S\left(\frac{\omega_o}{2}\right)$ is identical with the sum-function of Eq. (3.20).

First of the interesting results alluded to above is that $S\left(\frac{\omega_o}{2}\right)$ is always real; thus, if the imaginary part of $S(\omega)$ does not vanish at a frequency smaller than $\nu_o/2$, sampling-oscillations are the <u>only</u> possible oscillations of the system. This is because oscillation is not possible at frequencies greater than $\nu_o/2$, due to the translation property of the sampler output spectrum. The sampler output corresponding to an input having a period less than $2/\nu_o$ will have a spectrum line in the interval between zero and $\nu_o/2$ due to the first difference (i.e., the line $\nu_o - \nu < \nu_o/2$ if $\nu > \nu_o/2$). But this corresponds to an input of period $\frac{1}{(\nu_o - \nu)}$, greater than $2/\nu_o$; this signal will pass around the loop with its period unchanged (the loop is linear, aside from the sampler), and hence the oscillation could not have a period less than $2/\nu_o$. Thus, the sampling system can have no oscillation whose 'fundamental' frequency (reciprocal period) is greater than half the sampling frequency. This simplifies the task of evaluating $S(\omega)$ considerably, for one only need investigate the region $0 < \omega < \omega_o/2$, although this means evaluating the terms of S for all spectrum lines at frequencies for which G and W can be measured or computed.

4. EXPERIMENTAL VERIFICATION OF THE THEORY

4.1 Apparatus and methodology. The experiments were performed using a model sampler which was essentially a switch, which, when momentarily closed connected the input signal source to a storage capacitor, allowing the latter to charge by an increment of either sign, so as to take on the input signal voltage. The duration of the sampling 'instant' was approximately 4 microseconds.

'Droop' is an expression which describes the behavior of the sampler output as a function of frequency, due to the finite time-constant of the storage capacitor charging circuit. The effect is easily explained with reference to Fig. (4.1). G is the input signal source, whose internal impedance is represented by R_g. S is the switch, whose internal impedance is represented by R_s. C is the storage capacitor which effects the clamping action; Z_L is made as large as is practicable (e.g., the input impedance of a cathode follower). One seeks to make $R_g + R_s$ small enough, and leave S closed long enough, to allow V_c to come as close as possible to V_g; but one must compromise, lest there be an excessively low upper limit on usable frequency range, hence some value of 'sampling efficiency' less than unity must be tolerated.

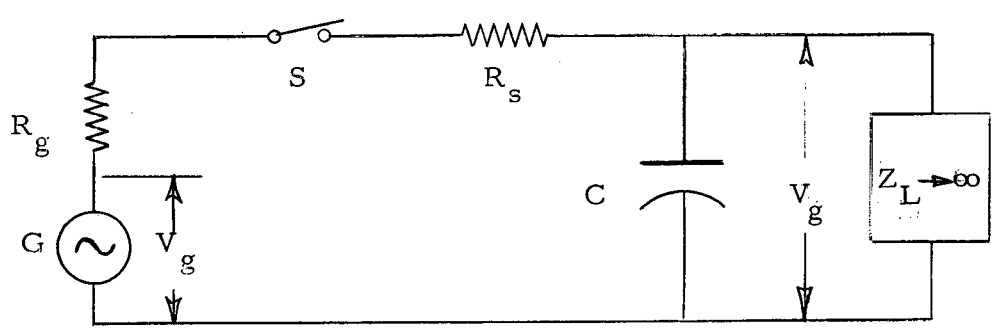

Fig. 4.1. The essential features of an amplitude sampler of the clamped type using a capacitive clamp.

The droop is symmetrical about $n\,\nu_o/2$, since it affects alike all spectral components of the output. In particular, interest here lies almost entirely in the region $0 \leq \nu \leq \nu_o$, hence one states that droop is symmetrical about $\nu_o/2$. Detailed discussion of droop, and derivation of the corrections applied to the data are carried out in Appendix I.

A schematic circuit diagram of the model sampler used in the experiments is shown in Fig. 4.2. The sampler model consisted of a bilateral gate, through which the signal from the input amplifier was impressed upon the storage capacitor during the gate-time. Gating pulse waveform is sketched in Fig. 4.2; the gating time was approximately 4 microseconds. Waveform of the output is also shown in Fig. 4.2. Gating pulses were obtained from a multivibrator-pulse amplifier chain, not shown in the figure. Amplitude of the gating pulses was approximately 110 volts; that of the output spikes was about 20 volts on the output cathode-follower grid. Rise-time of the output spike was about 1/2 microsecond.

4.2. Measurement of the transfer function. For this experiment the model sampler derived its input signal from a Hewlett-Packard model 650A signal generator operated at an output level of 0.10 volts rms. Sampler output was monitored on a Tektronix dc oscilloscope with amplitude measurements made with a Hewlett-Packard Model 300A spectrum analyzer.

In adjusting the data it was assumed that by far the largest error was due to 'droop' and that, at least in functional dependence upon frequency, any and all other effects contributed little to the errors. The droop correction factor ρ was determined by a least-squares reduction of the data between $\nu/\nu_o = 0.45$ and 0.55, where the "droop effect" was largest (see Appendix I). The data in this interval was thus adjusted by linear transformation to best fit the theoretical curve near $\nu_o/2$, and for this purpose fully half the data was taken in this interval.

In Fig. 4.3 is shown the data, as adjusted, compared with the function $\left|W(\nu/\nu_o)\right|$. Deviations range from +0.0126 to -0.0106, a total range of 0.0232. The average deviation is 0.00195 suggesting that the means of adjusting the data was reasonably objective. It is felt that the means was better than a least-squares adjustment over the entire domain of ν/ν_o, as the interval used in the adjustment calculation had about ten times the density of data as the remainder of the interval $0 \leq \nu/\nu_o \leq 1$. Average deviation

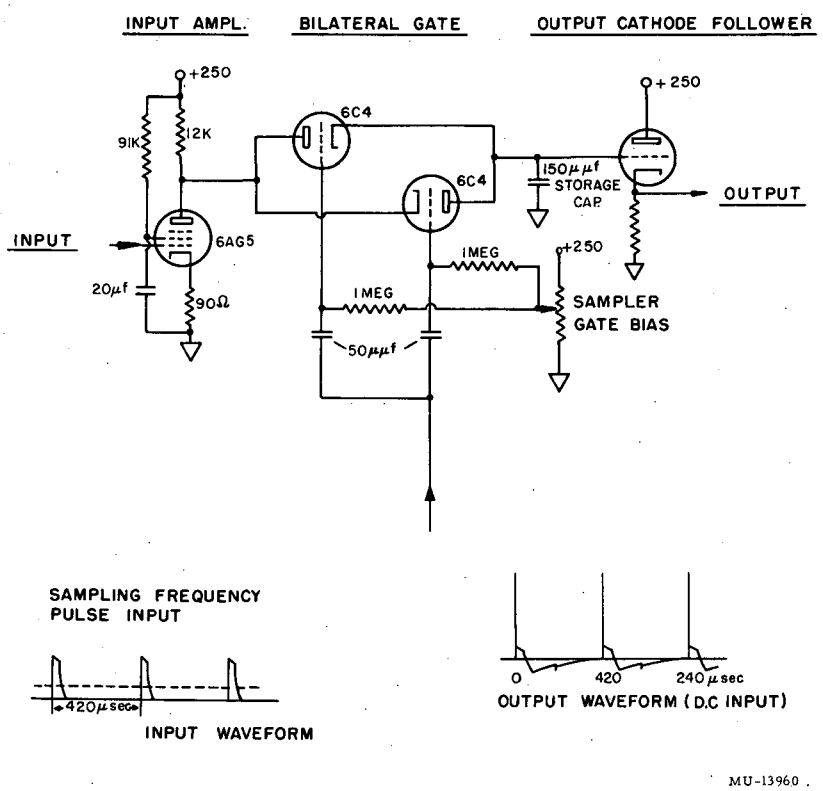

Fig. 4.2. Circuit diagram of model sampler used in experiments described in text.

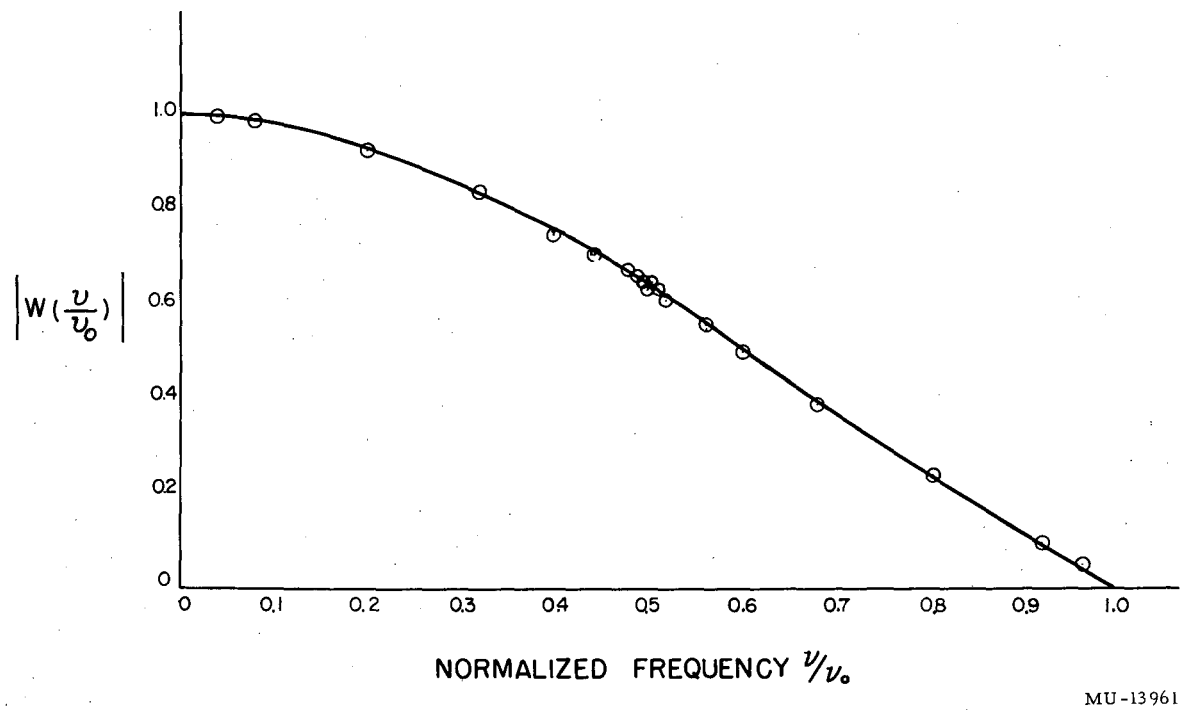

Fig. 4.3. Magnitude of transfer function of clamped sampler, with experimental points measured from model sampler.

in the adjustment interval was 10^{-4}, or 0.01%, which is the order of calculation errors in the numerical work. In the deviation interval ± 0.01 (1%), 82% of the data falls; all of it lies between ± 0.015. Inspection of the distribution plot suggests the latter figure as adequately expressing the maximum range of probable deviation (range of near certainty).

4.3. Spectral analysis experiment. Early in the course of this work several spectral analysis experiments were performed. These were done before the theory as it now stands was available, and were directed toward acquisition of knowledge regarding the nature of the sampling process. It was through these experiments that the sum-and-difference pattern of spectrum line frequencies was established experimentally, and moreover, that the effect called 'droop' was discovered.

There remained but one prediction of theory to be verified; namely the proposition that the same spectrum resulted from an input signal of unit amplitude having the frequency of any spectrum line. To prove this, data was taken with the same setup as was used for the measurement of the transfer function. The frequency $\nu/\nu_o = 0.10$ was chosen in order that 'droop' correction would be unnecessary. Sampling frequency was 2400 cycles sec^{-1}, making the lowest frequency (and largest amplitude) line occur at 240 cycles sec^{-1}.

The spectrum analyzer was adjusted so as to read 100 millivolts on the lowest line, with sampler input signal amplitude of 0.15 volts rms. The spectrum analyzer was then tuned to the frequency of the line to be observed, and peaked. The spectrum line frequency was considered as a parameter, with input frequency the independent variable. Thus the signal generator was tuned successively in increasing frequency to the frequency of each line in the spectrum, and the amplitude of the line being observed read from the spectrum analyzer. At the start of each run (i.e., whenever the spectrum analyzer was tuned to a new line frequency) the signal generator and spectrum analyzer were tuned to the frequency of the lowest line, and the analyzer re-normalized.

Data was tabulated in a square matrix array with input frequencies increasing to the right in columns, and spectrum line frequencies downward in rows. A similar matrix was tabulated for the deviations of the data from the normalized theoretical values. The deviations showed certain outstanding properties: firstly, the nondiagonal terms were small and of a consistent

magnitude. The data runs formed groups whose average deviations were all smaller than 0.003, and which averaged 0.0014. Sizes of the groups ranged from 0.001 to 0.004, the average being 0.0023. The deviations are plotted in Fig. 4.4. Theoretical amplitude of the smallest line observed (ν/ν_o = 4.9) was 0.020 for comparison.

Secondly among the noticeable properties of the terms in the deviation matrix was the periodicity of the group average deviation of nondiagonal terms. The average deviation for the lower frequency line in each order was, with only one exception, more positive than for the higher frequency line. The source of this effect was not tracked down, since the effect was very small and it was felt that emphasis should belong elsewhere.

The third property of the deviation matrix concerned the diagonal terms. These terms ran an order of magnitude larger than the nondiagonal terms, and showed the same periodicity (but of opposite sign) as mentioned above in connection with the nondiagonal data groups. Moreover, terms of each of the two signs, when plotted on a diagram similar to Fig. 4.4 fell very close to a smooth curve. This effect was not merely puzzling, but serious; therefore an effort was made toward accounting for it.

It was noted that the diagonal terms are those for which the input frequency is equal to the frequency of the spectrum line under observation. What happens if stray coupling exists which allows some of the input signal to couple directly to the output, doubtless with some phase-shift? If then the output spectral component of interest and the parasitic signal combine and interfere, one would expect very tangible deviations from theoretical values for these terms, and one would expect a strong frequency dependence.

Referring to Fig. 4.2, one sees a likely target for suspicion, namely the bilateral gate. There is approximately 2-1/2 μμf in tube capacitance, and some small amount of stray capacitance (order of 1 μμf) at this strategic point. It was decided to install some additional capacitance there and see what changes would occur. First 20 μμf was used, with profound effect. The deviations ran 100 times those for the nondiagonal terms, and again fell near smooth curves. Then the shunting capacitance was changed to 3 μμf, yielding deviations approximately twice those obtained with no shunting capacitance (see Fig. 4.5). At this time the cause of the anomalous behavior in the diagonal terms was felt to be apparent, and the subject dropped.

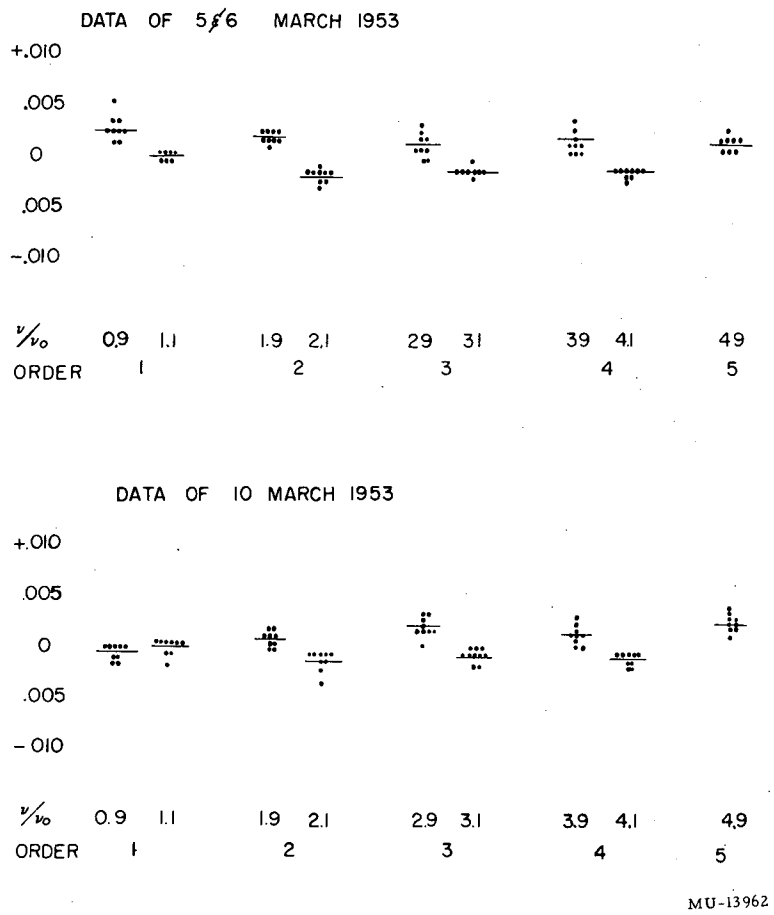

Fig. 4.4. Spectrum analysis experiment; deviation plots, nondiagonal terms. Data and theoretical values normalized to amplitude of the lowest frequency line (zero order). Amplitude of the smallest line observed is 0.020.

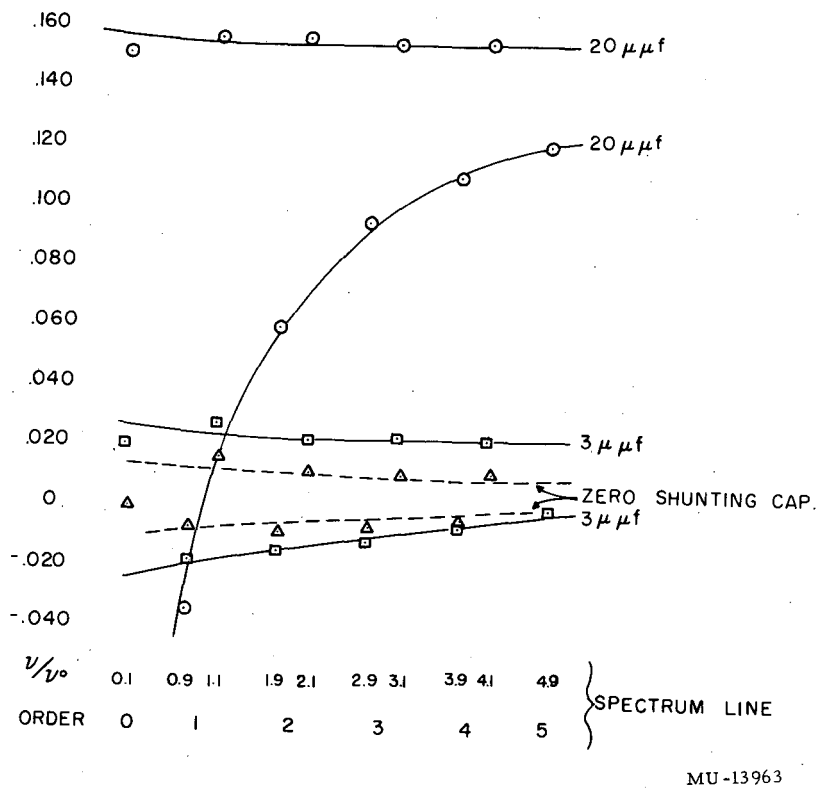

Fig. 4.5. Behavior of the diagonal terms of the deviation matrix shown as a function of the spectrum line measured. The parameter is shunting capacitance (in addition to strays) across the bilateral gate. Data and theoretical values were normalized to the amplitude of the lowest line of the spectrum ($\nu/\nu_o = 0.1$).

In light of the above, it is felt that the experiment was successful.

4.4. The closed-loop stability experiment. In order to verify the criterion for stability an experiment was designed which would meet two needs: (1) to involve sufficiently simple networks in the loop as to make possible a calculation of the oscillation condition by transient analysis, thus providing an independent calculation with which to compare results both of theory and of experiment, (2) to reduce the effect of intangible, or unaccountable variables to a minimum. Thus, there are derived three sets of gain values: (1) the results of application of Eq. (3.19), (2) the results of the transient analysis calculation, and (3) the results of experiment.

In the subsections to follow will be discussed the experiment, the methods of data reduction, the transient analysis calculations, the application of the stability criterion for sampling-oscillations, and a comparison of the results of the three independent determinations of the gain necessary to produce oscillations.

4.4.1. Description of the experiment. The simplest type of network suitable for attaining the objectives ennumerated above is one which involves a single energy-storage element. For convenience the capacitive phase-lag configuration was chosen. A schematic diagram of the apparatus is shown in Fig. 4.6. At the top of the figure are shown the sampler and the delay network, which was so designed that with convenient values of C, and of ν_o, three cases of RC could be measured: phase shift at $\nu_o/2$ to be approximately (1) $\pi/6$, (2) $\pi/3$, and (3) $5\pi/12$ (75°). The values of phase-shift used therefore corresponded roughly to normalized output amplitudes of (1) 1/2, (2) 1/3, and (3) 1/6. These values encompass a six-to-one range in bandwidth, and the results obtained illustrate the simplicity gained in the stability criterion with decreasing bandwidth, or saying it another way, they illustrate the complication introduced into the stability criterion when the bandwidth is made near to or greater than half the sampling frequency.

The return-path amplifiers are shown in the lower part of Fig. 4.6; they were so designed as to have a much larger bandwidth than that of the delay network at the lowest value of C used. A switch was provided in order that the loop might be opened or closed conveniently, with appropriate circuits arranged so as to maintain the necessary voltages at all

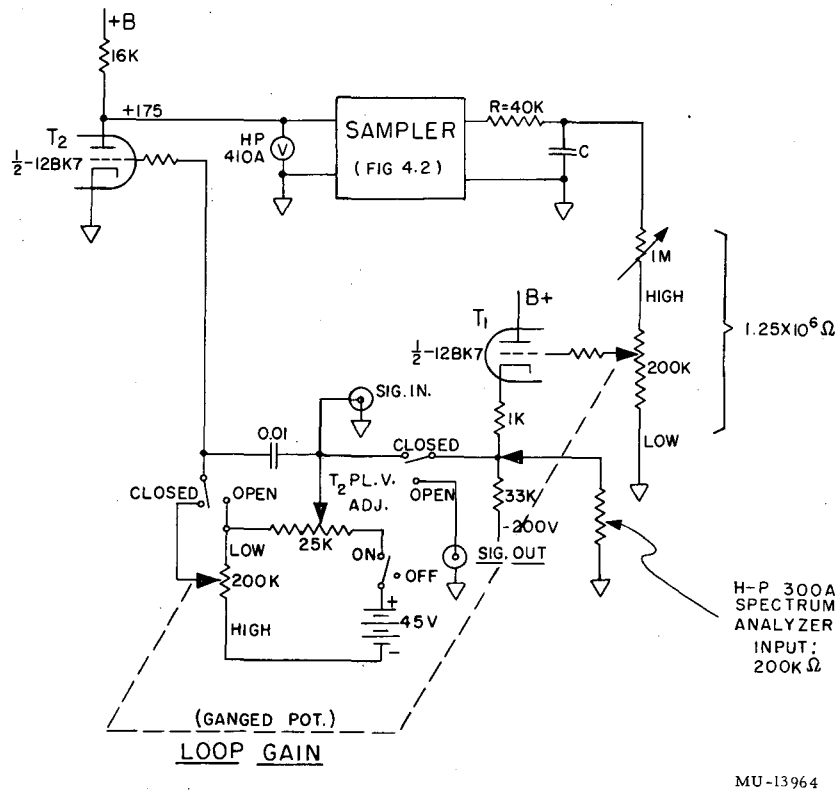

Fig. 4.6. Sampler - RC feedback apparatus, schematic diagram. Input of spectrum analyzer connected to "sig. in" when loop closed, and to "sig. out" when loop open. Effect is to have it shunted across the cathode-follower output at all times, as shown in diagram. Total (load) resistance shunting C is 1.25×10^6 ohms.

points regardless of whether the loop was closed or open, since it is of obvious importance that the gain of the system be precisely the same in either condition.

Figure 4.7 shows the apparatus in the closed-loop condition. It is to be noted that the Hewlett-Packard spectrum analyzer (model 300A), used in the gain measurements, was kept connected across the cathode-follower output in the closed-loop condition. The gain measurements were made in the open-loop condition, as shown in Fig. 4.8.

Using each of the three values of the capacitor C there were made several gain measurements. Firstly the loop was closed, and voltages were adjusted to the proper values; loop gain was raised very slowly until oscillations were imminent. The loop was then opened, voltages again read, and the gain measured. Preceding each loop closure the instrumental adjustments were checked carefully.

The measurements of gain were made at $\nu_o/10$, because of the spectrum analyzer bandwidth limitation. Measurements were made also at $\nu_o/2$, for checking purposes. It was assumed that in correction to zero frequency of the $\nu_o/10$ values the transfer function of the idealized delay network could be used without significant error. The sampling frequency was only 2400 cycles per second, hence the assumption that the transfer function of the apparatus below 240 cycles was ideal did not involve tangible risk!

The transfer function of the apparatus in the frequency range of zero to ν_o was measured experimentally. This was done in order that the actual apparatus could be replaced in the calculations by an 'ideal' model, but one in which the parasitic effects ('strays') were accounted for, through the use of experimentally measured parameters in the 'equivalent' network.

Measurements of the values of R and C used were made on a General Radio model 650A impedance bridge, the accuracy of which is stated by the manufacturer to be ± 1% at the values in question.

4.4.2. Data reductions. An inspection of Figs. 4.6, 4.7, and 4.8 will quickly assure the reader that although to a first order the loop frequency characteristic is that of a simple RC delay network, there can be expected a very tangible second-order correction, particularly in the wider-band conditions. This section will be devoted to a discussion of the more important parasitic effects,

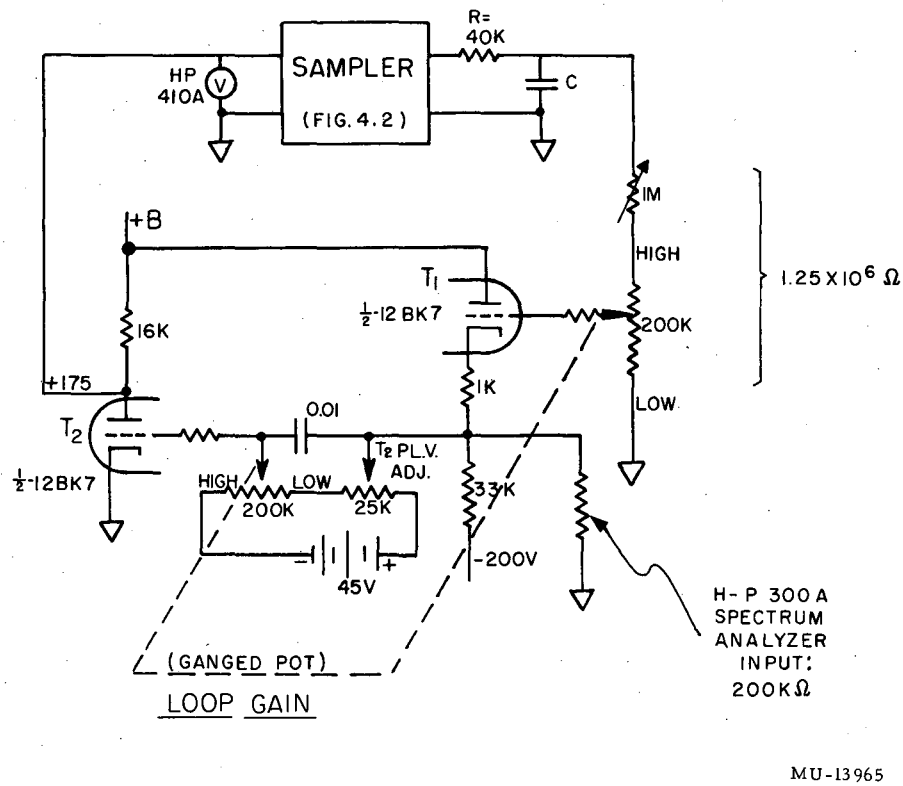

Fig. 4.7. Sampler - RC feedback apparatus: closed-loop simplified schematic.

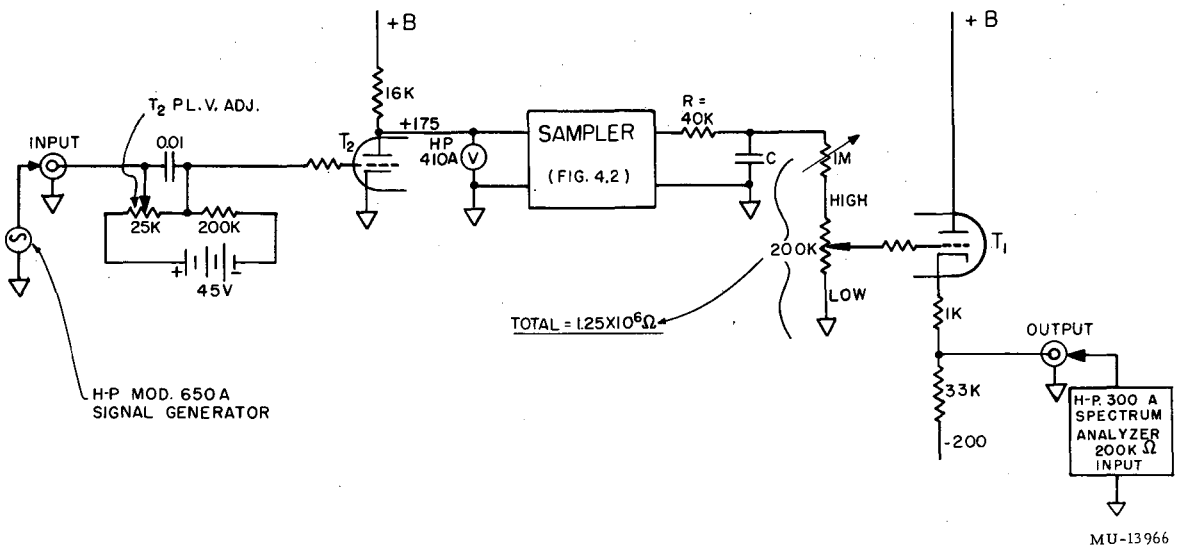

Fig. 4.8 Sampler - RC feedback apparatus: open-loop simplified schematic.

and the means of obtaining a second-order correction to the transfer function of the loop.

The most obvious effect is that of the output impedance, which was made purposely as large as feasible, with minimum capacitance. Since the accountable shunting capacitance can be placed in the order of 10^{-12} farad, it will not be explicitly considered. The equivalent network is thus shown in Fig. 4.9. The transfer function may be written down immediately, and simplifies to

$$v(\omega) = \frac{1}{(1 + r) + iCR\omega} \tag{4.1}$$

where $r = R/R'$, and

which is to be compared with the case wherein R' is infinite ($r = 0$)

$$v(\omega) = \frac{1}{1 + iCR\omega} \tag{4.2}$$

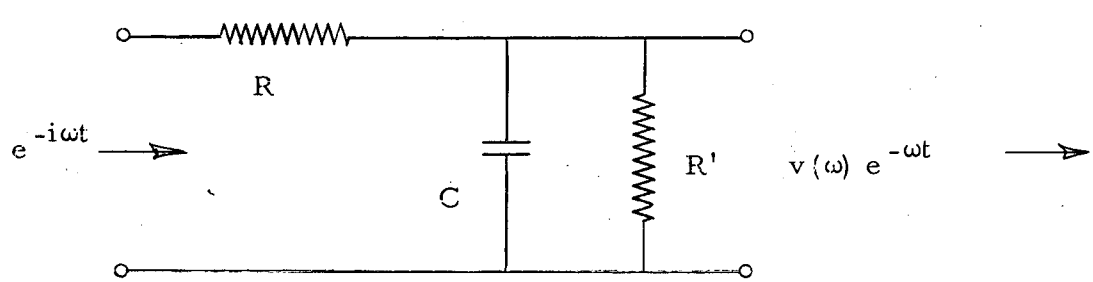

Fig. 4.9. RC delay network with output shunting resistance R'.

It is desirable to normalize the transfer functions to their zero-frequency values (making each the product of a gain constant and a frequency characteristic, or normalized transfer function). This is done for Eq. (4.1) by multiplying by (1 + r); thus,

$$v_o(\omega) = \frac{1}{1 + i\sigma'} \tag{4.3}$$

$$\sigma' = \frac{CR}{1 + r}\,\omega = \tau'\omega \tag{4.4}$$

whereas in the limiting case $r = 0$,

$$v_o(\omega) = v(\omega) = \frac{1}{1 + i\sigma} \tag{4.5}$$

$$\sigma = CR\omega = \tau\omega\,. \tag{4.6}$$

Therefore, it appears, the normalized transfer function of the shunted-output network is the same as that of the un-shunted one, provided one uses a 'corrected', or 'effective' resistance value $R/(1 + r)$.

There is, however, another effect to reckon with, namely the cumulative effect of all of the unaccountable parameters in the system, which become particularly troublesome when the wider bandwidths (smaller values of C) are used. As will be subsequently seen, even use of the 'corrected' resistance in the network calculation can lead to a demonstrably incorrect result. There is one way in which a correction may be introduced, and that is, to measure the transfer function experimentally and fit to that measurement a set of parameters of a suitable model. As things worked out, the authors were unable to do more than measure the amplitude of the transfer function for each value of C at nine values of frequency between zero and sampling frequency. These values, when plotted, gave curves essentially like the amplitude of Eq. (4.3) or (4.5), lying somewhat below the calculated 'model' curves. The experimental points were distributed about the average-curve in what seemed to be a fairly random manner. It was assumed that the equivalent network could be taken to be that of Fig. 4.8 without serious error, and that the time-constants τ (or τ') should be calculated by taking the

arithmetical average of the values of $\tau = \sigma/\omega$ obtained from the various amplitude measurements for each case. The values so obtained differed by very tangible amounts from the time-constants of the idealized networks, the differences being greater the smaller τ (greater bandwidth). This is as expected, and as noted above. The sizes of the discrepancies, however, are not comforting, and the assumption that the physical network differs from the 'equivalent' one by only a 'small' degree really generates only what could be called a 'first-order' correction. One interesting aspect of the problem is that the differences in the time-constants can be explained by increasing each of the values of C by approximately $4\ 1/2 \times 10^{-10}$ farad, which seems to indicate that at frequencies less than the sampling frequency the 'stray' effects appear as approximately 450 μμf of shunting capacitance across the output of the 'equivalent' network. Certainly at higher frequencies, however, stray inductances come into the picture, and phase-shifts certainly exceed $\pi/2$. Amplitudes, also, will be finite, but small, and the slowly-converging series which embodies the stability condition (Section 4.4.4) will not converge slowly enough to match the physical situation. These points will be illustrated in the comparison of results in Section 4.4.5.

4.4.3 Critical gain prediction by transient analysis. In view of the experimental limitations it is fortunate indeed that a network could be chosen whose properties make the feedback oscillations susceptible to simple analysis completely independent of the theory of Chapter 3. Indeed, agreement between two such independent calculations makes a resort to experiment unnecessary for the purpose solely of confirming a theory; the experimental results in this instance do serve a highly useful purpose, that of illustrating the importance of stray effects in the time-quantized feedback system, an importance quite out of proportion to that accorded strays in ordinary feedback practice.

The transient method is just that; one knows what the sampler output waveform is, and were he able to more readily solve a transient problem than to measure a transfer function the need for a frequency-domain stability criterion would not exist. It is seldom, however, that one can make time-domain measurements and calculations with the ease and certainty of those in the frequency domain.

Refer now to Fig. 4.10. Two waveforms are shown in superposition therein: they are the sampler output (square-wave, for the clamped case is being considered), and the sampler input, which is nothing more than the square-wave modified by the low-pass network and amplified. Consider now the time-sequence of events. At any given sampling instant, the network output has some value, say, $-y_o$ (which, amplified, provides the sampler input); sampling occurs, and the sampler output is clamped at its positive value, which we shall call unity. This is the input applied to the network of Fig. 4.9, whose output momentarily has the value $-y_o$. The network output (sampler input except for amplification) takes an exponential form, the asymptote being the network input (sampler output) value, unity. After the elapse of a sampling period, the sampler again samples and clamps, this time at some other value of voltage. The network output then beings to approach the new value on an exponential curve.

It is, of course, understood that the loop is oscillating at half the sampling frequency. Therefore, both waveforms are symmetric, and hence if the initial value of sampler input was $-y_o$, the alternate value is $+y_o$. Thus, in any sampling period $2nT < t < (2n + 1)T$, $y(t) = y_1(t)$, the output voltage of the network. In the next period, we call the network output $y_2(t)$; i.e., $(2n + 1)T < t < 2(n + 1)T$, $y(t) = y_2(t)$. The sampler output is said to oscillate between +1 and -1.

Then (see Fig. 4.10)

$$y_1(t) = -(1 + y_o)\, e^{-\frac{t}{\tau}} + 1$$

or,

$$y_1(t) = 1 - (1 + y_o)\, e^{-\frac{t}{\tau}} \tag{4.7}$$

and likewise

$$y_2(t) = (1 + y_o)\, e^{-\frac{t}{\tau}} - 1 \tag{4.8}$$

Now

$$y_1(T) = y_2(0) = y_o \tag{4.9}$$

and

$$y_2(T) = y_1(0) = -y_o \tag{4.10}$$

Equations (4.7) and (4.9), combined, give the same result as Eqs. (4.8) and (4.10), which is

$$y_o\left(1 + e^{-\frac{T}{\tau}}\right) = 1 - e^{-\frac{T}{\tau}} .$$

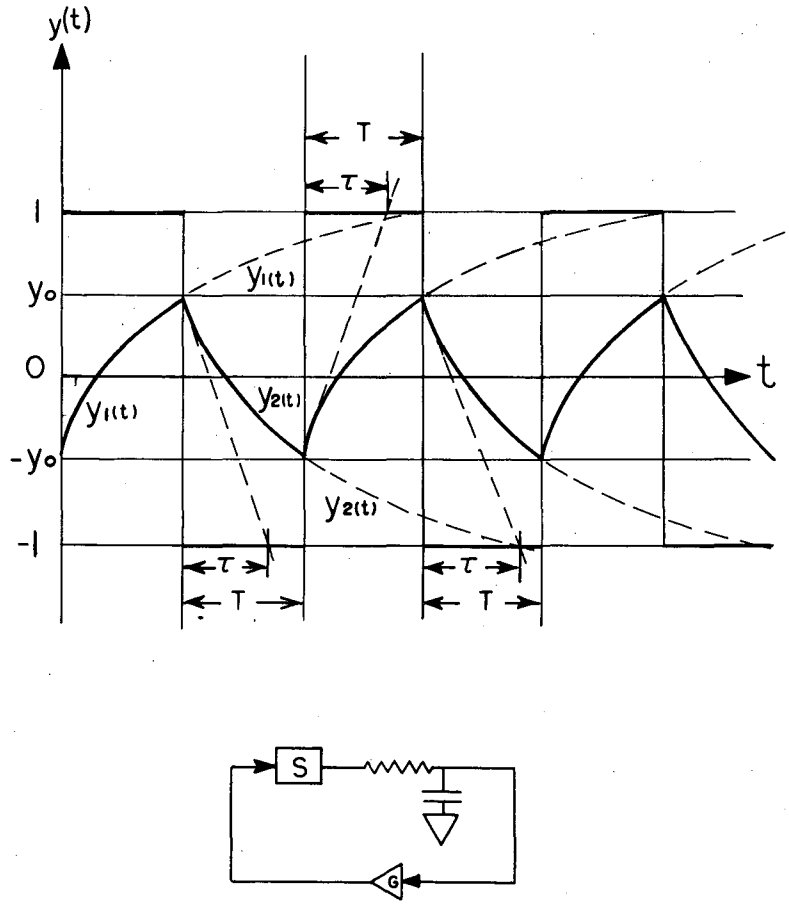

Fig. 4.10. Oscillations at half the sampling frequency in a feedback loop whose frequency properties are determined by a simple RC low-pass filter section.

Since the gain required to amplify the function y(t) to unit amplitude (in order that the sampled values are indeed unity) is just $1/y_o$; thus,

$$G(T,\tau) = \frac{1 + e^{-\frac{T}{\tau}}}{1 - e^{-\frac{T}{\tau}}} . \tag{4.11}$$

4.4.4. Application of the stability criterion. The application of the theory of Chapter 3 is very simply made. Using the notation of that chapter, and Eqs. (4.3) and (4.4) or (4.5 and 4.6),

$$G(\omega) = \frac{1}{1 + i\tau\omega} \tag{4.12}$$

so

$$X(\omega) = \frac{1}{1 + (\tau\omega)^2} \tag{4.13}$$

$$Y(\omega) = \frac{-\tau\omega}{1 + (\tau\omega)^2} . \tag{4.14}$$

Thus

$$Y\left(\left[2m-1\right]\frac{\omega_o}{2}\right) = \frac{-(2m-1)\frac{\tau\omega_o}{2}}{1 + \left[(2m-1)\frac{\tau\omega_o}{2}\right]^2} \tag{4.15}$$

Hence Eq. (3.21) becomes

$$\frac{1}{K} = \frac{4}{\pi}\left(\frac{2}{\tau\omega_o}\right) \sum_{m=1}^{\infty} \frac{1}{\left(\frac{2}{\tau\omega_o}\right)^2 + (2m-1)^2} \tag{4.16}$$

a very slowly-converging series indeed.

By direct application of a method due to Gumowski[13] the series of Eq. (4.16) can be accurately summed with the expenditure of a very modest effort, whereas, were the summation to be made term by term, calculations show that several hundred terms would be necessary. The results shown in

[13] Gumowski, I., "Summation of Slowly Converging Series", J.A.P. 24, 1068 (1953), letter.

the subsequent section as calculated from Eq. (4.16) were obtained in this way.

4.4.5. Tabulation and comparison of results. In Fig. 4.11 are represented the three experimental cases, each being characterized by a particular value of C. All three transfer functions are superposed, through the use of the dimensionless frequency variable, σ. The effect of strays is immediately apparent, and one would find it difficult to avoid entertaining doubts about the realism of the idealized transfer function at values of σ several times the sampling value; the problem is particularly acute when one considers the cumulative importance of the higher orders, as is indicated by the slowness of convergence of the series of Eq. (4.16).

In Table 4.1 the comparison is made numerically. Comparisons are made firstly of time-constant values, from which a low-frequency 'equilvalent' shunting capacitance was calculated, which seems remarkably consistent through the three cases, even though the time-constants cover an order of magnitude in range. Also tabulated are the values of $\sigma(\nu_o/2)$ (whose differences are, naturally, the same as those for the time-constant), and phase shift at $\nu_o/2$; it is these latter two which are shown explicitly in Fig. 4.11.

In Table 4.2 are exhibited for comparison the variously derived values for the loop gain required to produce the oscillations. As the primary standard of comparison we take the values calculated from transient analysis. With these the theory, as personified in Eq. (4.16), agrees perfectly. Since the networks used in the two calculations were the same (ideal networks), and since the transient-analysis approach must produce the correct value, one is justified in stating that the theory has met its test.

The experimental results are listed in the third and fourth columns of Table 4.2, the former being the gain values, the latter a comparison with the calculated values. It is instructive to compare these numbers in light of the approximate bandwidths, listed in column 5. Note that in case 3, where the bandwidth is approximately $\nu_o/8$, the strays are quite unimportant, whereas when the bandwidth is little more than doubled, the importance of the strays (through the higher orders of the spectrum) has increased more than five-fold. Some light into the specific nature of the effect the strays had upon the experimental results is shed by Fig. 4.12, which shows the transfer function of the entire feedback loop for case 1 (neglecting strays, excepting that the measured time-constants are used). The further effects of strays can be

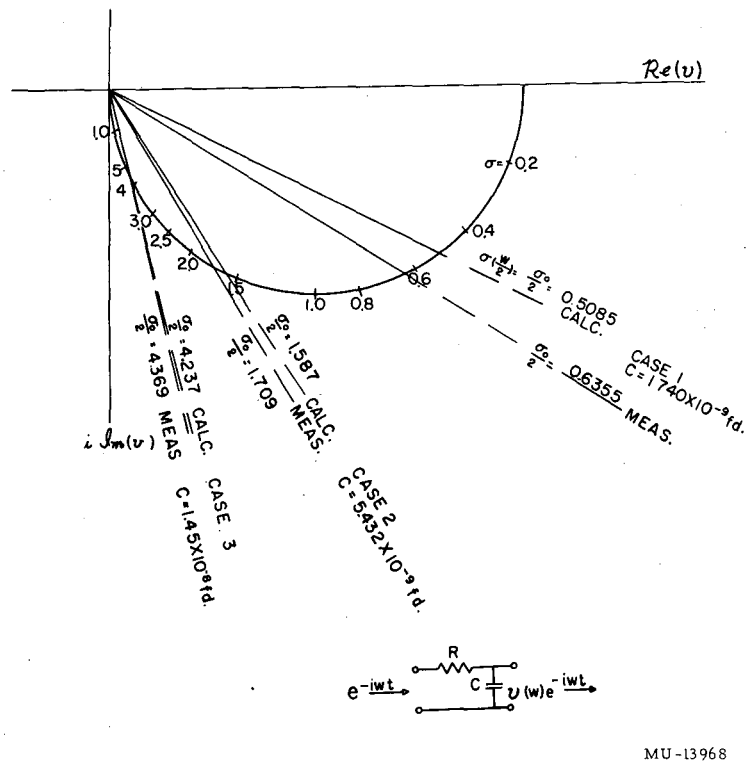

Fig. 4.11. Transfer function of RC delay network, frequency shown in terms of the dimensionless variable $\sigma = \pi\omega$. Shown here are the three cases for which critical closed-loop gain measurements were made at half the sampling frequency.

Note: Calculated values account for nothing more than the RC network plus its load resistance; measured values include entire apparatus. For technique and remarks re. limitations of the method, see text, Sec. 4.4.2.

Table 4.1. Parameters of Network 'Equivalent' of Feedback Loop in Stability Experiment

Case	C, farads (measured)	τ, seconds calculated	τ, seconds measured	Difference %	Shunt capacity 'equivalent' of difference
1	1.740×10^{-9}	6.744×10^{-5}	8.428×10^{-5}	+25	4.4×10^{-10} fd.
2	5.432×10^{-9}	2.105×10^{-4}	2.266×10^{-4}	+ 7.6	4.1×10^{-10}
3	1.45×10^{-8}	5.620×10^{-4}	5.794×10^{-4}	+ 3.1	4.5×10^{-10}

Case	$\sigma(\nu_o/2)$ calc.	$\sigma(\nu_o/2)$ meas.	$\sigma(\nu_o/2)$ diff. %	$\phi(\nu_o/2)$ calc. (degrees)	$\phi(\nu_o/2)$ meas. (degrees)	$\phi(\nu_o/2)$ diff. (degrees)
1	0.5085	0.6355	+25	26.95	32.4	+5.4
2	1.5874	1.709	+ 7.6	57.75	59.7	+1.9
3	4.237	4.369	+ 3.1	76.72	77.1	+0.4

Table 4.2. Comparison of Variously-Derived Values of Gain Required to Produce Sampling-Oscillations

Case	Gain required to produce oscillations Transient (Eq. 4.11)	Theory (Eq. 4.16)	Experimental	$\left(\frac{\text{meas.}}{\text{calc.}} - 1\right)$	Bandwidth (approximate)
1	1.058	1.058	1.24	+17.2%	$\frac{3}{2}$ $(\nu_o/2)$
2	1.438	1.438	1.56	+ 8.5%	$\frac{3}{5}$ $(\nu_o/2)$
3	3.028	3.028	3.07	+ 1.4%	$\frac{1}{4}$ $(\nu_o/2)$

expected to arise primarily in the influence of lead inductances, which will bring about additional phase-shifts in the higher orders. In Fig. 4.12 the interference circles for the first three orders (1st, 3rd, and 5th) are shown, and the partial sums of their intercepts. As well are shown the limits. Note that the measured value of critical gain is <u>less</u> than the calculated value; note further that the difference is roughly equal to the sum of <u>all</u> the orders above the fifth. Note also that the fifth order could have considerable additional phase-shift without affecting the results materially, i.e., the results are insensitive to a relatively small added phase-shift in the fifth order, but that any phase shift will be greatly magnified in the higher orders, and the contribution of any given order might well be zero, or positive. Indeed one might conclude, from the gain figures listed, and from the above, that the net effect of all of the higher orders is close to zero, indicating that about as many of the contributions were positive as were negative, or that the high-order parts of the transfer function were 'wrapped' around the origin by the effect of strays, instead of all lying on the same (negative) side.

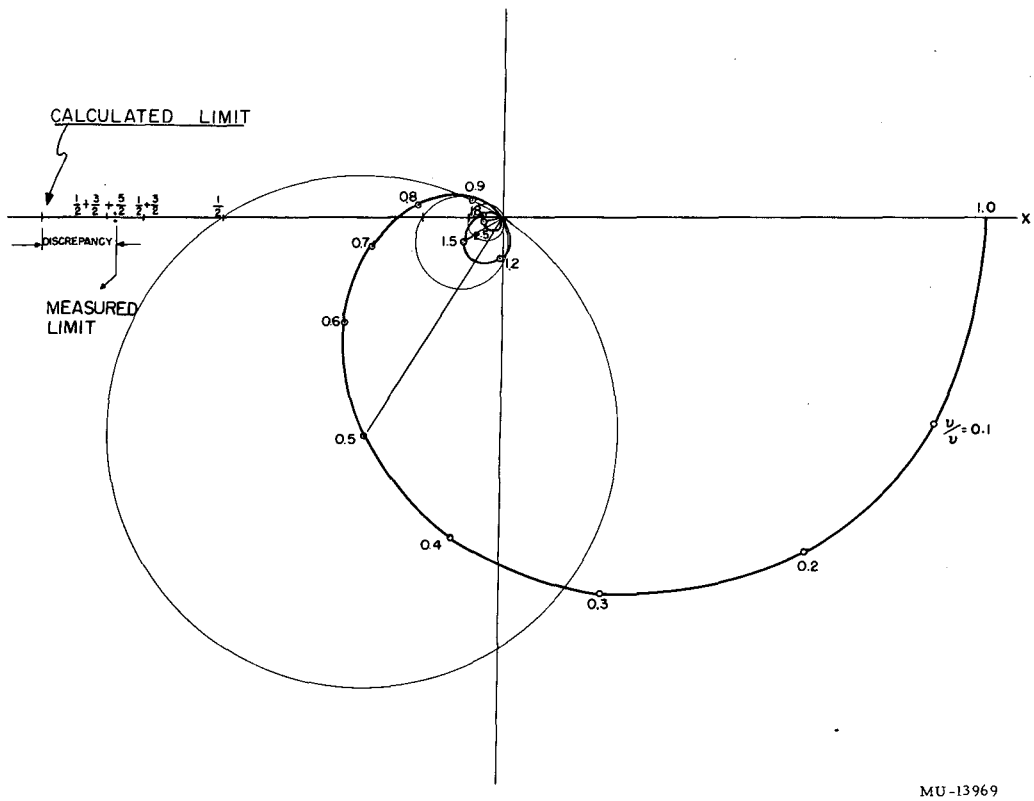

Fig. 4.12. Transfer function of feedback loop, case 1 (ideal network, measured value of τ) showing partial sums to order 5/2, and limits.

5. CONCLUSIONS

In the discussion concerning the properties of the output spectrum of a sampler, it was shown that a sampler can be regarded as having a transfer function, subject to certain definite limitations. This is due to the fact that the input spectrum appears in the output, with its components modified in amplitude and phase. The sampling process is an essentially nonlinear one, in that new spectrum lines are generated, but it was shown that no interaction effects occur between input components (i.e., that there is no intermodulation, or 'mixing').

The transfer function is continuous, excepting at multiples of half the sampling frequency. The existence of such a transfer function makes possible the use of Nyquist's criterion for stability, so extended as to account for the complexity of the waveform of feedback oscillations, when they exist. The peculiar behavior of the transfer function at multiples of $\nu_0/2$ is due to interference between the spectral components of those frequencies.

Since previous publications in this field have included no more than an occasional bare mention of sampling-oscillations, the subject was treated in complete detail here; the extension of Nyquist's stability criterion implied by Linvill was shown to include the case of sampling-oscillations.

The extension of Nyquist's criterion is embodied in the application of the criterion in the customary manner, not to the loop transfer-function, but to a sum-function (see Eq. 3.30) which embodies the contributions to the sampler input waveform of all the spectral orders in the sampler output, as modified by the loop transfer-function. It was seen that the sum-function evaluated at half-sampling frequency is always real, with the implication that if this sum-function does not become real (and negative) at any frequency below half-sampling, the only oscillations which the system can have are the sampling-oscillations. No oscillations can ever occur with a period shorter than twice the sampling period, because of the transposition of spectra in the sampling process. Thus, in stability calculations, no base frequencies above half-sampling need be used. However, terms for the sum-function must be calculated (or scaled graphically) from the transfer-function of the loop (including sampler) for spectral orders as high as can be calculated (or scaled) considering the number of significant figures in the calculation. Indeed, the sum-function may be a very slowly converging series, in which case any graphical estimate of critical gain is a rough one, and must include some sensible accounting of high-frequency 'stray' effects.

When the loop is subject to sampling-oscillations, the critical gain can be roughly estimated by simple graphical means. The procedure is as follows (see Fig. 4.12): (1) plot the transfer function of the entire loop, including sampler, (2) place the compass point on the point of the transfer function corresponding to the frequency $m \frac{\omega_o}{2}$ (m an odd integer), (3) set the compass so as to pass a circle through the origin, (4) strike an arc across the real axis, so as to indicate the intercept of the mth order circle on the real axis, (5) repeat for every order for which amplitude of the transfer function is sufficient to allow the construction, (6) add these algebraically (easily done with a scale), and (7) mark off the sum on the real axis. That is the critical point for sampling-oscillations. If it is on the positive real axis, or if it lies on the negative real axis inside the continuous portion of the transfer function, sampling-oscillations cannot occur, and the conventional Nyquist criterion provides the limitation. Note that the estimate is only that, since the cumulative effect of the neglected orders may be quite noticeable.

6. ACKNOWLEDGMENT

The authors wish to acknowledge with gratitude the contribution of their friend and colleague, Dr. Bob H. Smith, who kindly consented to read the manuscript. From Dr. Smith's criticisms came certain distinct improvements in the text, most notably in the Introduction.

The authors further wish to gratefully acknowledge the encouragement given by George M. Farly during the course of this work.

APPENDIX I

Waveform Factor of a Capacitively Clamped Sampler ('Droop')

As has been stated previously, the sampler with a capacitive clamp is essentially a capacitor charged through a switch or gate. The input signal is assumed to be slowly varying when referred to the gating interval as a unit of time. The gating interval, or time interval during which the switch is closed, is a constant, and is in most cases exceedingly small in comparison with the sampling period $1/\nu_o$. During the gating interval, the capacitor (C_1 of Fig. 3.1) charges to some fraction, η, of the difference between the input voltage during the gating interval, and the voltage to which the capacitor had previously been charged. If the period of a sampled signal, having a given amplitude, were many sampling periods long, the increments in sampled voltage would be small, and the failure of the output to follow the input (i.e., the voltage error generated in the charging process) would be a certain (small) fraction of the amplitude of the sampled signal. If, however, the sampled signal has a frequency of near $\nu_o/2$, the voltage excursions between sampling instants will be near the maximum possible value, and the voltage error generated will be a much larger fraction of the amplitude of the sampled signal. Thus, droop must be a function of frequency. Furthermore, considering the symmetry of the output spectrum (as a function of input frequency) about $\nu_o/2$, this voltage error must be symmetrical about $\nu_o/2$.

One is here faced with a choice of making a complete analytical approach or of attacking the task in a piecewise manner. Since this effect accounts at most for a correction of a few percent, and the objective is to achieve a reasonable first-order correction, the latter method was chosen; the first would present a mathematical problem formidable indeed, and the result for the present purpose is hardly worth a fraction of the effort.

The problem will be solved in three parts; firstly a point at $\nu_o/2$ can be calculated to good approximation, secondly, one at $\nu_o/4$. Lastly, an expression can be derived for frequencies much less than $\nu_o/4$. This gives sufficient data for the desired correction curve: in the interval $0 \leq \nu \leq \nu_o/2$. Symmetry fills out the interval to ν_o.

Case where $\nu/\nu_o << 1/4$:

Consider a monotone increasing function, with argument t, and let the domain of t be subdivided into equal intervals by a sequence of points $\{t_k\}$. Let the values of the function, which we call $f(t)$, be, on the set $\{t_k\}$

$$f(t_k) = f_k \tag{I-1}$$

which form a monotone increasing sequence. Let a sequence $\{F_k\}$ correspond to f_k through the sampling process, subject to the limitations outlined in the first paragraph of this appendix. Figure I-1 illustrates the case. For any interval we have

$$F_k = F_{k-1} + \eta(f_k - F_{k-1})$$

or

$$F_k = F_{k-1}(1 - \eta) + \eta f_k \tag{I-2}$$

Let $f_o = 0$, which may in any case be realized by a linear transformation. Then,

$$F_1 = \eta f_1$$

Substituting in (I-2) we have for $k = 2$

$$F_2 = \eta\left[(1 - \eta) f_1 + f_2\right]$$

iterated substitution into (I-2) gives the result

$$F_k = \eta\left[f_k + (1-\eta)f_{k-1} + (1-\eta)^2 f_{k-2} + \ldots (1-\eta)^{k-1} f_1\right] \tag{I-3}$$

Thus, after k steps the normalized amplitude is

$$\frac{F_k}{f_k} = \eta\left[1 + (1-\eta)\frac{f_{k-1}}{f_k} + (1-\eta)^2\frac{f_{k-2}}{f_k} + \ldots (1-\eta)^{k-1}\frac{f_1}{f_k}\right] \tag{I-4}$$

Since f_k is monotone increasing, $f_{k-p}/f_k \leq 1$ for $0 \leq p \leq k$. Suppose that $1-\eta << 1$, then,

$$F = \frac{F_k}{f_k} \cong \eta\left[1 + (1-\eta)\frac{f_{k-1}}{f_k}\right] \tag{I-5}$$

The bigger the last jump, the smaller the correction term, hence the smaller the output (larger droop). For $k = 1$ (1 step) $F_k/f_k = \eta$, and for an indefinitely refined subdivision, F_k/f_k approaches unity. In any event, the last jump has the most influence on the outcome, and the more gentle the slope near the end point, the closer F_k/f_k is to unity. Physically, this is because the capacitor has more chances to charge to the desired final value.

For sinusoidal input, $f(t)$ is a sinusoidal segment, the portion lying in the interval $(0,\pi/2)$. One changes the frequency by changing k, the normalized output being

$$F \cong \eta \left[1 + (1-\eta) \sin \left(\frac{k-1}{k} \frac{\pi}{2}\right)\right] \qquad \text{(I-6)}$$

Case where $\nu/\nu_o = 1/2$:

Referring to Fig. I-2, we denote by x the equilibrium amplitude of the square wave; by inspection

$$2x = \eta(1 + x)$$

so

$$x = \frac{\eta}{2 - \eta} \qquad \text{(I-7)}$$

write (I-7) as

$$x = \frac{\eta}{1 + \rho}$$

letting $\rho = 1-\eta$.

Then $x = \eta\left[1 - \rho + \rho^2 \ldots\right]$; to the first order, for $\rho << 1$,

$$x = \eta(1-\rho)$$

or

$$x \cong (1-\rho)^2; \text{ to the first order, noting that } x=F(1/2)$$

or

$$F(1/2) = 1 = 2\rho \qquad \text{(I-8)}$$

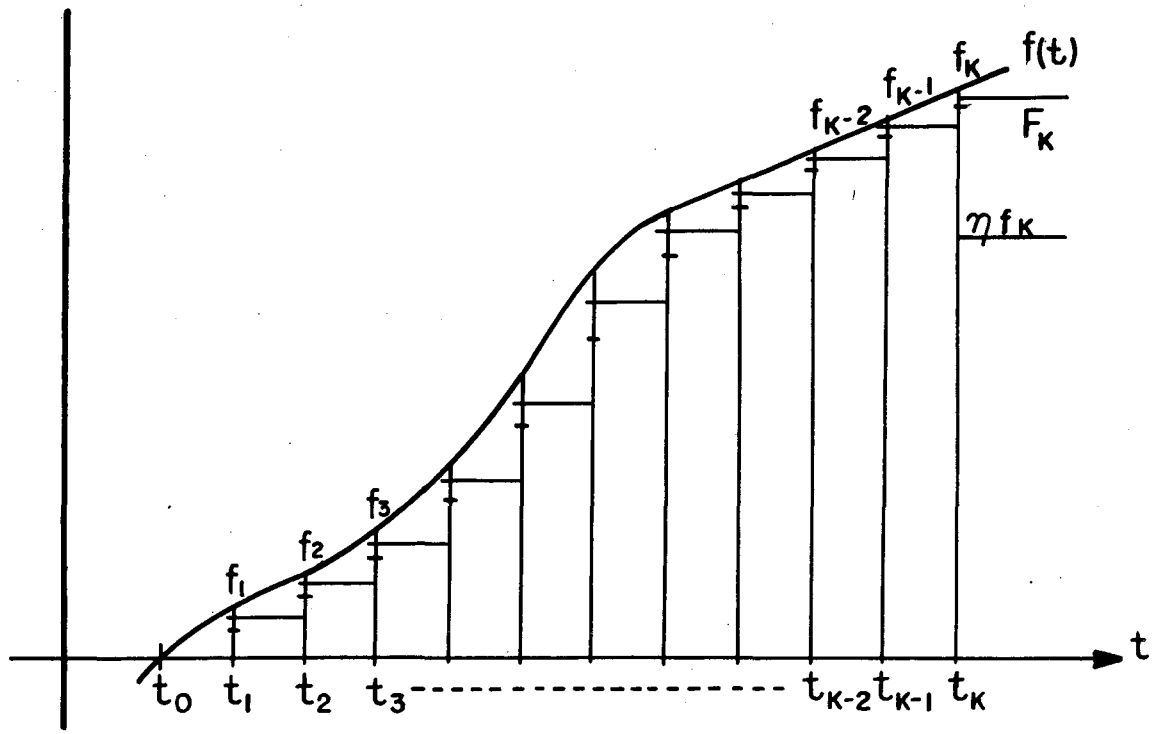

MU-13949

Fig. I-1. Sampling process, showing the origin of "droop" or waveform factor, using the value $\eta = 3/4$ to emphasize the result.

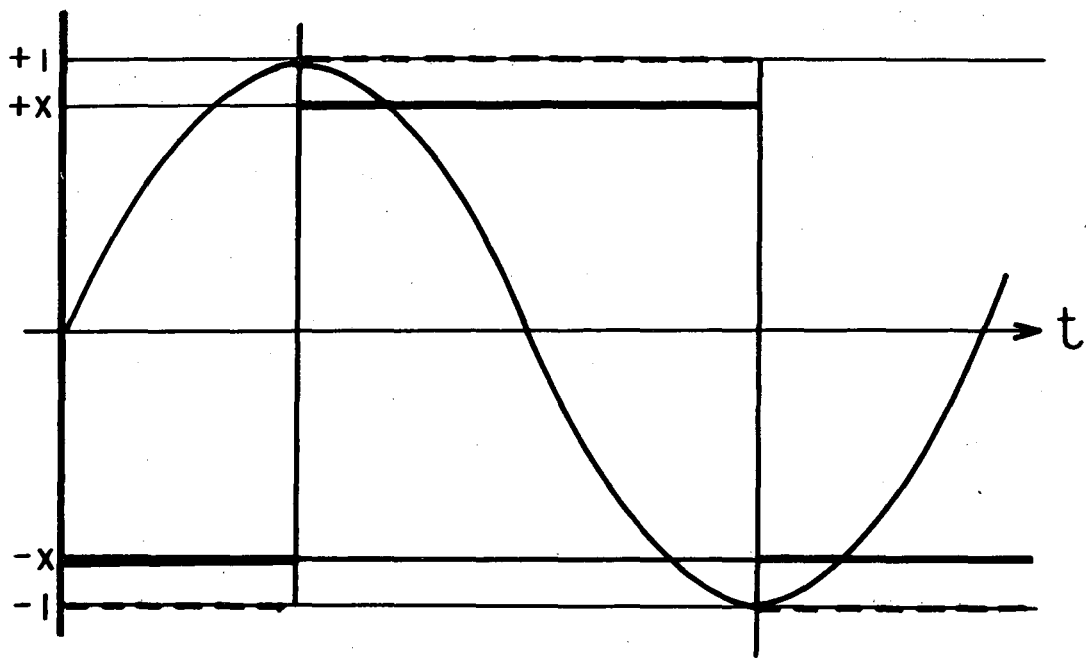

MU-13950

Fig. I-2. Sampling process for $\nu/\nu_o = 1/2$; x is the equilibrium value of the square-wave.

Case where $\nu/\nu_o = 1/4$:

Referring to Fig. I-3, we denote by x the maximum excursion of the waveform, i.e., 1-x is the measure of failure to attain the sampled value when that value is unity (maximum), and by y we denote the minimum excursion, or the failure of the waveform to return to the axis when the sampling 'instant' occurs at a zero of the input.

Again by inspection we write

$$x = \eta(y + 1)$$
$$y = \eta(1 - x)$$

by mutual substitution these yield

$$x = \frac{\eta(1 + \eta)}{1 + \eta^2} \qquad \text{(I-9)}$$

$$y = \frac{\eta(1 - \eta)}{1 + \eta^2} \qquad \text{(I-10)}$$

again letting $1-\eta = \rho$ we have

$$1 + \eta^2 = 1 + (1-\rho)^2$$
$$\cong 2(1-\rho)$$

Then

$$x \cong \frac{1 + \eta}{2}$$

or to the first order,

$$x = 1 - \rho/2 \qquad \text{(I-11)}$$

likewise,

$$y = \rho/2 \text{ again to the first order.} \qquad \text{(I-12)}$$

Now resolve the output waveform into the sum of two like waveforms, one of amplitude x, the other of amplitude y, these being mutually phased at a quarter period (Fig. I-4). Each of these can be analyzed as the sum of two square-waves phased at half a period. When the fundamental-frequency components of these waveforms are combined, with due regard for phase and compared with the case $x = 1$, $y = 0$ (no droop) there is the result, to the first order,

$$F(1/4) = 1 - \frac{\rho}{2} \qquad \text{(I-13)}$$

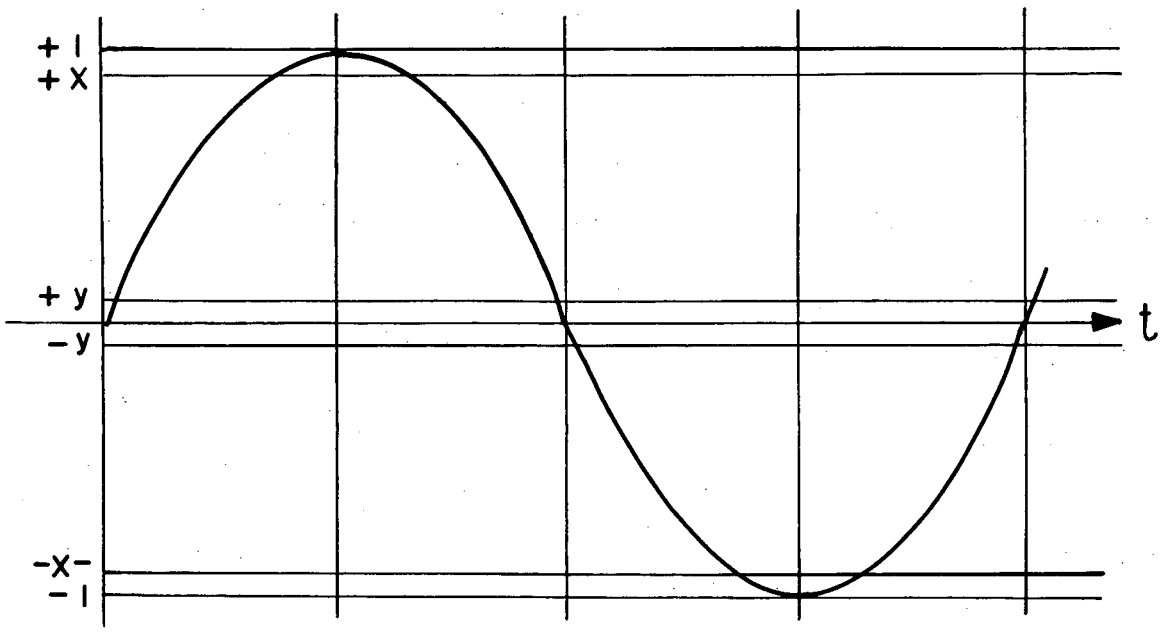

MU-13951

Fig. I-3. Sampling process for $\nu/\nu_o = 1/4$, with heavy line showing the equilibrium output.

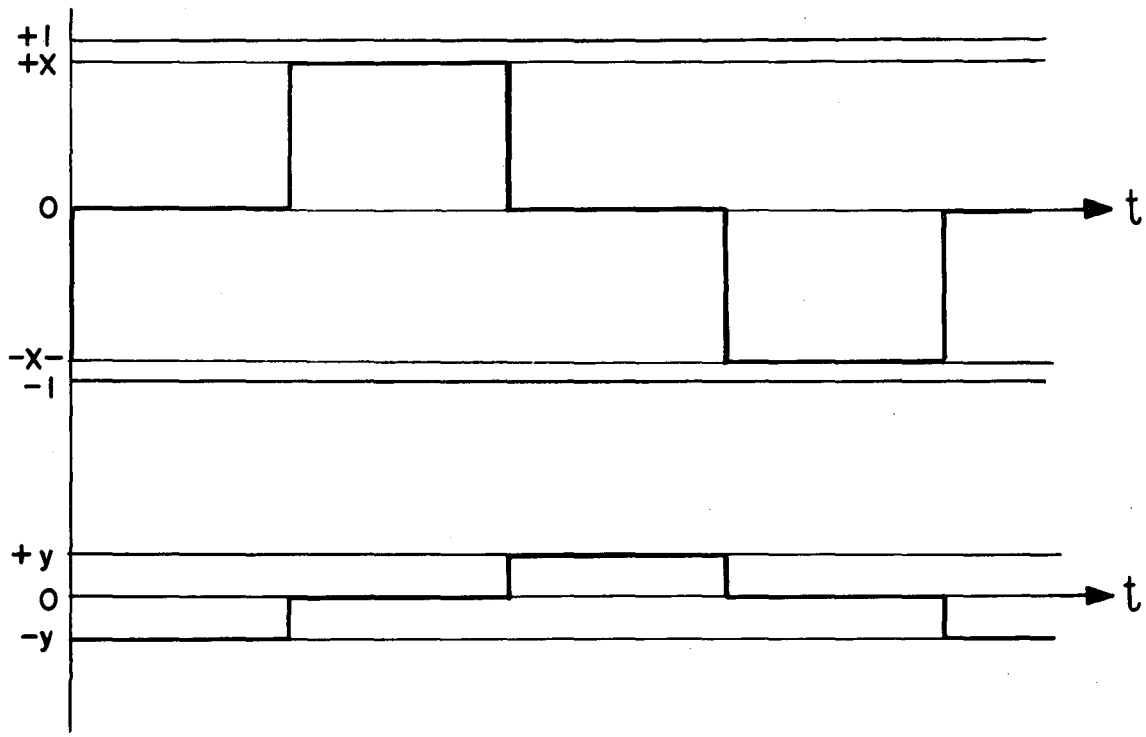

MU-13952

Fig. I-4. Resolution of waveform of Fig. I-3 into component similar waveforms.

From the above results, points were calculated for arguments of 1/40, 1/12, 1/8, 1/4, and 1/2.

These points are plotted in Fig. I-5. Together with the point at zero the sequence excepting the points at 1/12 and 1/8 falls upon a smooth curve. The two latter points were deemed to have been poorly approximated by the formula, Eq. (I-6).

It is of course necessary to somehow determine the value of ρ for a given physical sampler. This was done by means of the least-squares adjustment of the data in the neighborhood of $\nu_o/2$, which resulted in acceptance of the value $\rho = 0.021$ for the sampler used in the experiment. Droop at $\nu/\nu_o = 1/2$ (maximum) is 4.2%. The data was adjusted by use of the curve of Fig. I-5, with the results as discussed in the text.

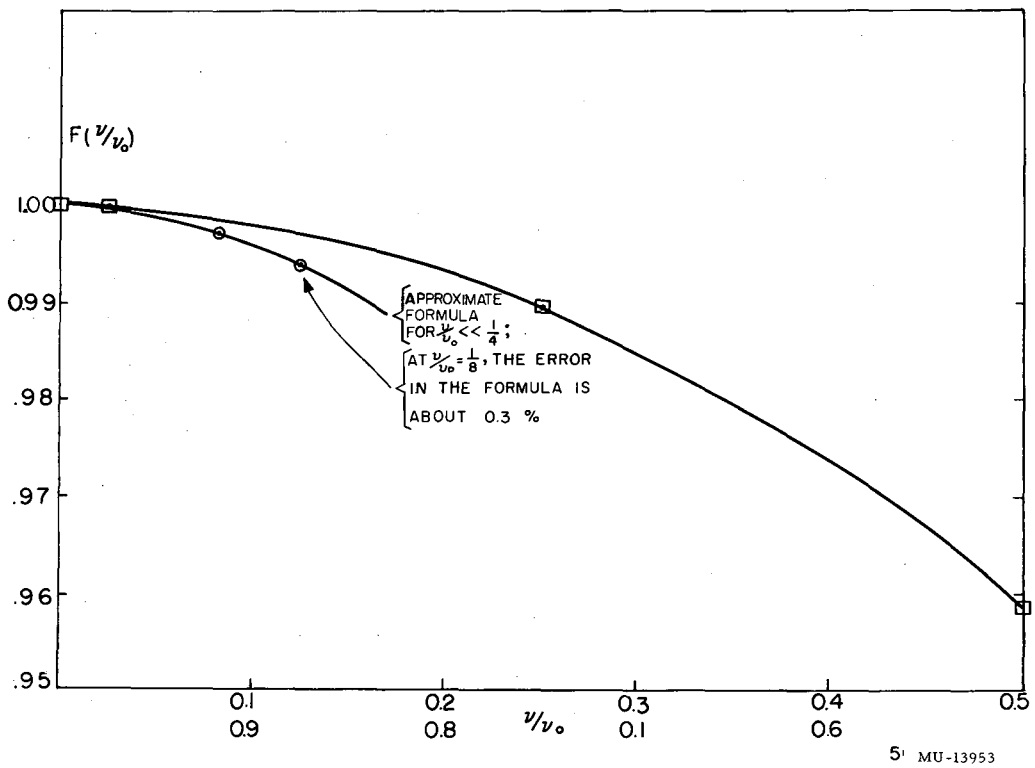

Fig. I-5. Waveform factor of a clamped sampler having a sampling "efficiency" of 0.958 ("droop" of 4.2%).
⊡ points calculated from valid approximations
⊙ points calculated from failing approximations, not trusted.